We are IntechOpen, the world's leading publisher of Open Access books Built by scientists, for scientists

6,900
Open access books available

186,000
International authors and editors

200M
Downloads

Our authors are among the

154
Countries delivered to

TOP 1%
most cited scientists

12.2%
Contributors from top 500 universities

WEB OF SCIENCE™

Selection of our books indexed in the Book Citation Index in Web of Science™ Core Collection (BKCI)

Interested in publishing with us?
Contact book.department@intechopen.com

Numbers displayed above are based on latest data collected.
For more information visit www.intechopen.com

Chapter 15

Airlift Bioreactors: Hydrodynamics and Rheology Application to Secondary Metabolites Production

Ana María Mendoza Martínez and
Eleazar Máximo Escamilla Silva

Additional information is available at the end of the chapter

http://dx.doi.org/10.5772/53711

1. Introduction

The bubble column and airlift bioreactors are pneumatically agitated and often employed in bioprocesses where gas-liquid contact is important. The role of the gas is to provide contact with the liquid for mass transfer processes such as absorption or desorption and to provide energy through gas expansion or bubble buoyancy for liquid mixing. In these two pneumatically agitated reactors, gas is sparger usually through the bottom and the buoyancy of the ascending gas bubbles causes mixing. The main difference between these two pneumatically agitated reactors is in their fluid flow characteristics. The flow in the airlift is ordered and in a cyclic pattern like in a loop beginning from top through to bottom. The airlift differs from the bubble column by the introduction of inner draft tubes which improves circulation, whereas the bubble column is a simple tower. In the airlift, liquid recirculation occurs due to the four distinct sections; the riser, downcomer, gas separator and bottom or base. The bubble column is a simple vessel without any sectioning making the flow rather a complex one.

Some attractive features of the airlift are the low power consumption, simplicity in construction with no moving parts, high mass and heat transfer rates and uniform distribution of shear [1, 2].

The advantage of its low power consumption is of particular importance in effluent (e.g. wastewater) treatment where the product value is comparatively low. Therefore, operational cost (efficient use of energy) is greatly considered since corresponding applications are usually on a large scale. Homogenous shear is particularly important for biological processes that are shearing sensitive. In the conventional stirred tank, shear is greatest at the stirrer and decreases away from it to the walls of the vessel. This creates a gradient of shearing which can have

INTECH
open science | open minds

© 2013 Martínez and Silva; licensee InTech. This is an open access article distributed under the terms of the Creative Commons Attribution License (http://creativecommons.org/licenses/by/3.0), which permits unrestricted use, distribution, and reproduction in any medium, provided the original work is properly cited.

adverse effect on the morphology or sometimes can damage cells (e.g. animal and plant cells). The simple construction of the airlift without shafts makes it not only aesthetically pleasing to look at but also eliminates contamination associated with the conventional stirred tank which is a major drawback in the production of microorganism. A sterile environment is crucial for growing organisms especially in the bioprocesses since contamination reduces product quality, generates wastes, also more time and money are spent to restore the whole process.

In addition to the previously described, the development of new biotech products: drugs, vaccines, tissue culture, agrochemicals and specialty chemicals, biofuels and others have had a major breakthrough during the last decade. But engineering to scale these developments to the production phase is lagging far behind in advances in the efficient development of bioprocesses. Normally these processes are complicated because they are conducted in complex systems, three or four phases, microorganisms that are susceptible to large shear produced by stirring; require high airflow rates, and changes in rheology and morphology cultures through the time. The soul of a bioprocess is still the bioreactor, since it determines the success of a good separation and therefore the cost of the product. In this chapter we describe one of the most promising bioreactors for their processing qualities, good mixing, low shear, easy to operate with immobilized microorganisms, low consumption of energy, we are talking about the airlift bioreactors. In this context the parties will start from basic engineering bioreactors: mass balances, mass transfer, and modelling and to cover the hydrodynamics and rheology of the process. Finally we will present two cases of application on the production of Bikaverin (a new antibiotic), and L-lysine.

2. Hydrodynamic characteristic of airlift reactors

Fluid mixing is influenced by the mixing time and gas holdup which defines the fluid circulation and mass transfer properties. The fluid recirculation causes the difference in hydrostatic pressure and density due to partial or total gas disengagement at the gas separator (top clearance, *tt*). Studies have been documented during the last two decades with various correlations applicable for hydrodynamic parameters [3-5]. This implies that for a successful design, fundamental understanding of mixing parameters is important for industrial scale-up.

It is difficult to generalize the performance of the bioreactor according to the process for which the airlift will be employed. For example, in aerobic fermentation, oxygen is important for mass transfer and therefore, it is imperative to consider a design where there will be less disengagement of gas resulting in higher gas holdup for a higher mass transfer rate. In this case, the liquid circulation velocity is low because less gas is disengaged at the top resulting in a lower differential density. Furthermore, other processes require good mixing other than a high mass transfer rate. However, provision can be made by increasing the gas disengagement at the top to improve the liquid recirculation as in the case for anaerobic fermentation. Therefore, it is safe to conclude as have been confirmed [3, 6, 7] that, the geometry parameters such as the top clearance (*tt*), ratio of cross sectional area of the downcomer to the riser (*Ad*/*Ar*), bottom clearance (*tb*), the cross sectional areas of riser (*Ar*) and that of the downcomer

http://dx.doi.org/10.5772/53711

(*Ad*), draft tube internal diameter (*Dd*), and height of the column (*H*) and superficial gas velocity *(Ug*) have an influence on fluid hydrodynamics.

There is extensive information on the measurement of fluid hydrodynamics published with a handful of equations. However, most of them Gumery et al.: Characteristics of Macro-Mixing in Airlift Column Reactors 7 Published by The Berkeley Electronic Press, 2009 cannot be correlated due to the different medium (Newtonian versus non-Newtonian) used and various assumptions made. The different measuring techniques often used cannot discriminate diffusion and convection for mixing whiles others disturb process flow.

On the other hands the interconnections between the design variables, the operating variables, and the observable hydrodynamic variables in an airlift bioreactor are presented diagrammatically in Figure 4 as has been reported by [8]. The design variables are the reactor height, the riser-to-downcomer area ratio, the geometrical design of the gas separator, and the bottom clearance (C_b, the distance between the bottom of the reactor and the lower end of the draft tube, which is proportional to the free area for flow in the bottom and represents the resistance to flow in this part of the reactor). The main operating variables are primarily the gas input rate and, to a lesser extent, the top clearance (C_t, the distance between the upper part of the draft tube and the surface of the non-aerated liquid). These two independent variables set the conditions that determine the liquid velocity in the airlift bioreactor via the mutual influences of pressure drops and holdups, as shown in Figure 1 [9]. Viscosity is not shown in Figure 1 as an independent variable because in the case of gas–liquid mixtures, it is a function of the gas holdup (and of liquid velocity in the case of non-Newtonian liquids), and because in a real process, it will change with time due the changes in the composition of the liquid.

3. Flow configuration

3.1. Riser

In the riser, the gas and liquid flow upward, and the gas velocity is usually larger than that of the liquid. The only exception is homogeneous flow, in which case both phases flow at the same velocity. This can happen only with very small bubbles, in which case the free-rising velocity of the bubbles is negligible with respect to the liquid velocity. Although about a dozen different gas–liquid flow configurations have been developed [10], only two of them are of interest in airlift bioreactors [11, 12]:

1. Homogeneous bubbly flow regime in which the bubbles are relatively small and uniform in diameter and turbulence is low.
2. Churn-turbulent regime, in which a wide range of bubble sizes coexist within a very turbulent liquid.

The churn-turbulent regime can be produced from homogeneous bubbly flow by increasing the gas flow rate. Another way of obtaining a churn-turbulent flow zone is by starting from slug flow and increasing the liquid turbulence, by increasing either the flow rate or the

diameter of the reactor, as can be seen in Figure 5 [12]. The slug-flow configuration is important only as a situation to be avoided at all costs, because large bubbles bridging the entire tower cross-section offer very poor capacity for mass transfer.

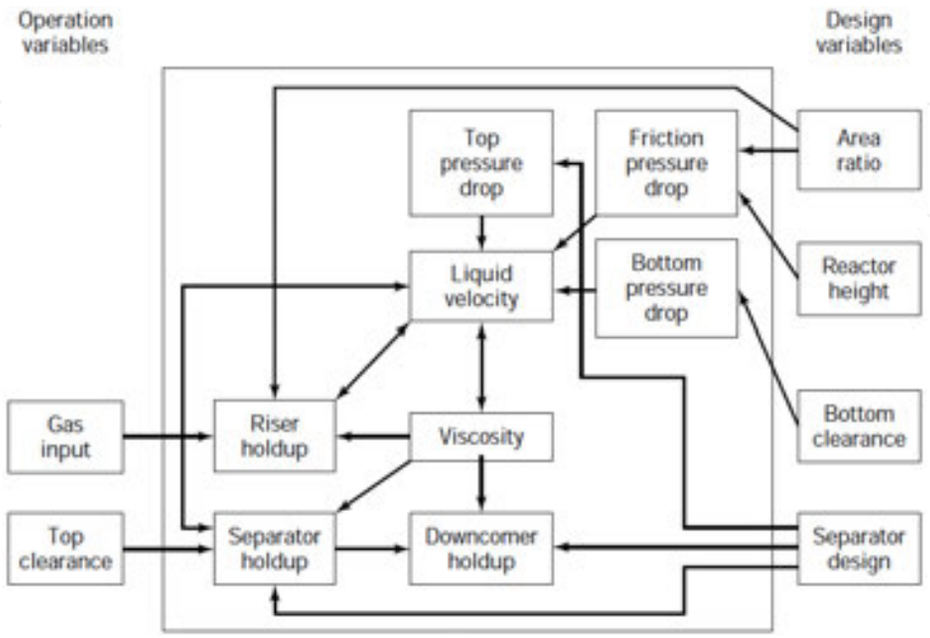

Figure 1. Interaction between geometric and fluid dynamic variables in an airlift bioreactor [9].

3.2. Downcomer

In the downcomer, the liquid flows downward and may carry bubbles down with it. For bubbles to be entrapped and flow downward, the liquid velocity must be greater than the free-rise velocity of the bubbles. At very low gas flow input, the liquid superficial velocity is low, practically all the bubbles disengage, and clear liquid circulates in the downcomer. As the gas input is increased, the liquid velocity becomes sufficiently high to entrap the smallest bubbles. Upon a further increase in liquid velocity larger bubbles are also entrapped. Under these conditions the presence of bubbles reduces the cross-section available for liquid flow, and the liquid velocity increases in this section.

Bubbles are thus entrapped and carried downward, until the number of bubbles in the cross-section decreases, the liquid velocity diminishes, and the drag forces are not sufficient to overcome the buoyancy. This feedback loop in the downcomer causes stratification of the bubbles, which is evident as a front of static bubbles, from which smaller bubbles occasionally escape downward and larger bubbles, produced by coalescence, escape upward. The bubble front descends, as the gas input to the system is increased, until the bubbles eventually reach the bottom and recirculate to the riser. When this point is reached, the bubble distribution in the downcomer becomes much more uniform. This is the most desirable flow configuration in the downcomer, unless a single pass of gas is required. The correct choice of cross-sectional area ratio of the riser to the downcomer will determine the type of flow.

http://dx.doi.org/10.5772/53711

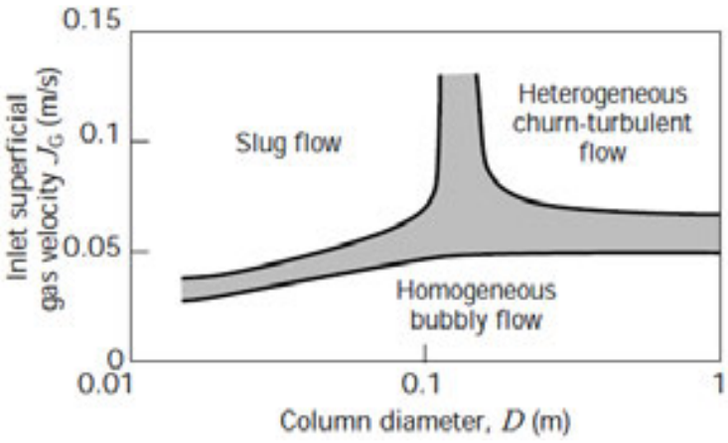

Figure 2. Map of flow configurations for gas–liquid concurrent flow in a vertical tube [12].

3.3. Gas separator

The gas separator is often overlooked in descriptions of experimental airlift bioreactor devices, although it has considerable influence on the fluid dynamics of the reactors. The geometric design of the gas separator will determine the extent of disengagement of the bubbles entering from the riser. In the case of complete disengagement, clear liquid will be the only phase entering the downcomer. In the general case, a certain fraction of the gas will be entrapped and recirculated. Fresh gas may also be entrapped from the headspace if the fluid is very turbulent near the interface. The extent of this entrapment influences strongly gas holdup and liquid velocity in the whole bioreactor.

It is quite common to enlarge the separator section to reduce the liquid velocity and to facilitate better disengagement of spent bubbles. Experiments have been reported in which the liquid level in the gas separator was high enough to be represented as two mixed vessels in series [13]. This point will be analysed further in the section devoted to mixing.

4. Gas holdup

Gas holdup is the volumetric fraction of the gas in the total volume of a gas–liquid–solid dispersion:

$$\varphi_1 = \frac{V_G}{V_L + V_G + V_S} \tag{1}$$

where the sub-indexes L, G, and S indicate liquid, gas, and solid, and *i* indicates the region in which the holdup is considered, that is, gas separator (s) the riser (r), the downcomer (d), or the total reactor (T).

The importance of the holdup is twofold: (a) the value of the holdup gives an indication of the potential for mass transfer, since for a given system a larger gas holdup indicates a larger gas–

liquid interfacial area; and (b) the difference in holdup between the riser and the downcomer generates the driving force for liquid circulation. It should be stressed, however, that when referring to gas holdup as the driving force for liquid circulation, only the total volume of the gas is relevant. This is not the case for mass transfer phenomena, in this case, the interfacial area is of paramount importance, and therefore some information on bubble size distribution is required for a complete understanding of the process.

Because gas holdup values vary within a reactor, average values, referring to the whole volume of the bioreactor, are usually reported. Values referring to a particular section, such as the riser or the downcomer, are much more valuable, since they provide a basis for determining liquid velocity and mixing. However, such values are less frequently reported.

The geometric design of the airlift bioreactor has a significant influence on the gas holdup. Changes in the ratio $\frac{A_d}{A_r}$, the cross-sectional areas of the downcomer and the riser, respectively, will change the liquid and gas residence time in each part of the reactor and hence their contributions to the overall holdup. Gas holdup increases with decreasing $\frac{A_d}{A_r}$, [14-17].

4.1. Gas holdup in internal airlift reactors

Correlations presented for internal-loop airlift bioreactors are shown in Table 1. These take into account liquid properties and geometric differences within a particular design. Most of the correlations take the form:

$$\varphi_r = a(J_G)^{\alpha}\left(\frac{A_d}{A_r}\right)^{\beta}(\mu_{ap})^{\gamma} \tag{2}$$

where φ_r is the gas holdup in the riser, J_G is the superficial gas velocity (gas volumetric flow rate per unit of cross sectional area), μ_{ap} is the effective viscosity of the liquid, and α, β, γ, and a are constants that depend on the geometry of the reactor and the properties of the liquid. The correlation can be used to predict the holdup in a system that is being designed or simulated as a function of the operating variables, the geometry of the system, or the liquid properties. Such correlations are effective for fitting data for the same type of reactor (e.g., a split-vessel reactor) with different area ratios or even different liquid viscosities, but they are mostly reactor-type specific.

The cyclic flow in the airlift bioreactor complicates the analysis of the system. The riser gas holdup depends strongly on the geometric configuration of the gas–liquid separator and the water level in the gas separator. This has been shown experimentally in a split-vessel rectangular airlift bioreactor [18], but the premise can essentially be extended to any internal loop airlift bioreactor. Analysis of the system revealed that these factors influence the gas disengagement and hence the gas recirculation in the downcomer. When this influence is taken into account and the holdup is plotted against the true gas superficial velocity, J_G, true, which is defined as the sum of the gas superficial velocity due to the freshly injected gas, Qin, and to the recirculated gas, Q_d, that is,

http://dx.doi.org/10.5772/53711

$$J_{G,\,true} = \left(\frac{Q_{in} + Q_d}{A_r}\right) \tag{3}$$

Then all the data for the different gas separators may be represented by a single relationship, such as equation 3. In other words, if the actual gas flow is known, the influence of gas recirculation (which depends on $\frac{A_d}{A_r}$, and the design of the gas separator) has been airlift bioreactor ready taken into account and does not need to be considered again. Nevertheless, this simple approach has a drawback in that the true gas superficial velocity is difficult to measure because the gas recirculation rate is usually not known. Thus, correlations that take into account all the variables, which may be easily measured, remain the option of choice. Table 1 shows most of the correlations of this type that have been proposed for the riser holdup in internal loop Airlift bioreactors. Comparison of a number of these correlations shows that there is reasonable agreement between the predictions of the different sources. Figure 1 can be used as an example of the actual state of-the-art in airlift bioreactor design. A number of correlations have been proposed, and three variables ($\frac{A_d}{A_r}$, l_{ap}, and J_G) have been tested by most researchers. The ranges in which these variables were studied vary from source to source.

In addition, some other variables (such as bottom clearance, top clearance or gas separator design, and surface tension) have been used by some authors but ignored by others. One example is the disengagement ratio defined by Siegel and Merchuk [19], which represents the mean horizontal path of a recirculating bubble relative to the external diameter and is equivalent to the parameter obtained by dimensional analysis [1] as:

$$M = \frac{D_S}{4D} \tag{4}$$

where D is the diameter of column and D_s the diameter of gas separator. If this parameter is not taken into account, then studies of the influence of the top clearance [13, 20] are incomplete and difficult to extrapolate to other designs.

The same can be said about the filling factor [21] given by the ratio of the gas separator volume to the total volume.

The foregoing discussion thus explains why all the correlations coincide for some ranges of these secondary variables while in other ranges they may diverge. In addition, in some cases the number of experiments may not have been sufficient to provide correlations or they may have been ill-balanced from the statistical point of view. The obvious solution to this problem lies in the collection of a large and detailed bank of reliable data that will constitute the basis for correlations with greater accuracy and validity. The safest procedure for the prediction of the gas holdup in an airlift bioreactor under design is to take data provided by researchers who have made the measurements in that particular type of reactor with the same physico-chemical properties of the system. If this option is not available, then correlation 9 in Table 1 [17], is recommended for prediction of the gas holdup in the riser.

Gas holdup in the downcomer is lower than that in the riser. The extent of this difference depends mainly on the design of the gas separator [22]. The downcomer gas holdup is linearly dependent on the riser holdup, as a consequence of the continuity of liquid flow in the reactor.

Many expressions of this type have been published [3]. At low gas flow rates, u_d is usually negligible, since most of the bubbles have enough time to disengage from the liquid in the gas separator. This usually happens at the low gas flow rates frequently used for animal cell cultures.

The gas holdup in the separator is very close to the mean gas holdup in the whole reactor [1] as long as the top clearance C_t is relatively small (one or two diameters). For larger top clearances, the behaviour of the gas separator begins to resemble that of a bubble column, and the overall performance of the reactor is influenced by this change.

In our laboratory we had some studies on the production of some secondary metabolites like phytohormones and protein hydrolysis, amino acid production, xanthophyll and new antibiotics. The next part of this chapter shows two cases were we try to show the applications of air lift bioreactors from various viewpoints, such as hydrodynamics, rheology and engineering aspects themselves. So to provide some useful engineering tools when these bioreactors takes to consideration:

5. Case 1: Hydrodynamics, mass transfer and rheological studies of Bikaverin production in an airlift bioreactor

5.1. Introduction

Antibiotics are small chemical agents (m.w. 600-800 Daltons) designed to eliminate harmful bacteria. They are produced from yeasts of fungi and bacteria. The first antibiotic discovered was penicillin in 1928/29 The first therapeutic application was in 1940 by Florey and Chain, during the Second World War when the need for antibiotics was increasing. Antibiotics belong to a group of substances called secondary metabolites. These substances appear to be unrelated to the main process of growth and reproduction. Good producers of secondary metabolites possess weak regulation of primary metabolism and visa-versa. Antibiotics are produced in limited substrate and oxygen conditions. They are produced to provide some protection against competing species in critical growth conditions. The starting points for antibiotic production are mainly amino acids and acetyl CoA with isoprene and shikimic acid also being involved. Antibiotic production commences at some point in differentiation often during sporulation. Process development consists essentially of modifying the metabolic system so that diversion of the material and biosynthesis are greatly increased. No cell growth or reproduction occurs during antibiotic production as the energy produced is being used to produce the antibiotic so that the cell can survive in the limited substrate.

After the discovery and first use of antibiotics the productivity and product concentration was increased by development of better strains or by improvement of the reaction conditions such

http://dx.doi.org/10.5772/53711

1	$\varphi_r = 0.44\ f_{G_r}^{0.841} \mu_{ap}^{-0.135}$ $\varphi_d = 0.297\ f_{G_r}^{0.935}$
2	$\varphi_r = 2.47\ f_{G_r}^{0.97}$
3	$\varphi_r = 0.465\ f^{0.65}\left(1 + \frac{A_d}{A_r}\right)^{-1.06} \mu_{ap}^{-0.103}$
4	$\varphi_r = 0.65\ f^{(0.603+0.078C_o)} \left(1 + \frac{A_d}{A_r}\right)^{-0.258}$ $\varphi_d = 0.46\varphi_r - 0.0244$
5	$\varphi_r = \left(0.491 - f_{G_r}^{0.706}\right) \left(\frac{A_d}{A_r}\right)^{-0.254} D_r \mu_{ap}^{-0.068}$
6	$\varphi_r = 0.16 \left(\frac{J_{Gr}}{J_{1r}}\right)^{0.57} \left(1 + \frac{A_d}{A_r}\right)$ $\varphi_d = 0.79\varphi_r - 0.057$
7	$\varphi_r = 0.364\ J_{Gr}$
8	$\frac{\varphi_r}{1 - \varphi_r} = \frac{J_{G_r}^{n+2/2(n+1)}}{2^{3n+1\ n+1n} \left\| {}^{n+2}\right/ {}_{2(n+1)} \left(\frac{K}{\rho_1}\right)^{1/2(n+1)} g^{n/2(n+1)} \left(1+\frac{A_d}{A_r}\right)^{3(n+2)/4(n+1)}}$
9	$\frac{\varphi}{(1 - \varphi)^4} = \frac{0.124\left(\frac{J_G \mu_1}{\sigma_1}\right)^{0.996} \left(\frac{\rho_1 \sigma_1^3}{g \mu_1^4}\right)^{0.294} \frac{D_r}{D}^{0.114}}{1 - 0.276\left(1 - e^{-0.0368 M_a}\right)}$
10	$\varphi_r = \frac{F_r}{0.415 + 4.27\left(\frac{J_{Gr} + J_{1r}}{\sqrt{g D_r}}\right)\left(\frac{g\rho_1 D^2}{\sigma_1}\right)^{-0.188} + 1.13 F_r^{1.22} M_o^{0.0386} \left(\frac{\Delta\rho}{\rho_1}\right)^{0.0386}}$
11	$\frac{\varphi}{(1 - \varphi)^4} = 0.16 \left(\frac{J_{Gr}}{\sigma_1}\mu_1\right) M_o^{-0.283} \left(\frac{D_r}{D}\right)^{-0.222} \left(\frac{\rho_1}{\Delta\rho}\right)^{0.283} + \left(1 - 1.61\left(1 - e^{-0.00565 M_a}\right)\right)$
12	$\varphi_d = 4.51 \times 10^6 M_o^{0.115} \left(\frac{A_r}{A_d}\right)^{4.2} \varphi_r$ When $\varphi_r < 0.0133\left(\frac{A_d}{A_r}\right)^{-1.32}$ and $\varphi_d = 0.05 M_o^{-0.22}\left[\left(\frac{A_r}{A_d}\right)^{0.6} \varphi_r\right]^{0.31 M_o^{-0.0273}}$ When $\varphi_r > 0.0133\left(\frac{A_d}{A_r}\right)^{-1.32}$
13	$\varphi_r = 0.0057\left[(\mu_1 - \mu_w)^{2.75} - 161\frac{73.3 - \sigma}{79.3 - \sigma}\right] . f_{G_r}^{0.88}$
14	$\varphi_r = \frac{0.4 F_r}{1 + 0.4 F_r\left(1 + \frac{J_1}{J_{Gr}}\right)}$
15	$\varphi = 0.24 n^{-0.6} F_r^{0.84 - 0.14n} G_a$

Table 1. Gas Hold-Up in Internal-Loop airlift bioreactors

as substrates and process controls. There was also a change from surface cultures to batch stirred tank reactors with complex media. The next step was the introduction of the fed batch configuration, which extended the length of the production phase and avoided repression during high substrate levels.

For maximum yield we have to design a process that only minimally involves the primary metabolism.

The main function of a properly designed bioreactor is to provide a controlled environment in order to achieve optimal growth and/or product formation. In this review we will look at the bioreactor design and the factors that are available in producing high yields of antibiotics. In general bioreactor design, the growth kinetics of the microorganism plays a key role in determining the type of reactor. Factors include; yield coefficients and maintenance requirements, the exponential, stationary and lag phase kinetics, and the formation of growth and non-growth associated product production formation. Due to the constraints of the report, these factors are largely ignored and the main focus is on gaining knowledge on reactor configuration on the maximum yield of general antibiotics.

In our laboratory after work of ten years in research the optimal production of gibberellins we found that the *Gibberella fujkuroi* produce a potent antibiotic named Bikaverin. Bikaverin is a red pigment with specific anti-protozoal activity against *Leishmania brasiliensis* and anti-tumour activity. Additionally, bikaverin and its derivatives have a cytotoxic effect on in vitro proliferating cells of Erlich ascites carcinoma, Sarcoma 37 and leukaemia L-5178 and is a fermentation product of *Gibberella fujikuroi* or *Fusarium sp*. The formation of bikaverin precedes that of gibberellin [23] and both secondary metabolites are produced from the primary metabolite acetyl-CoA. Bikaverin is synthesized via the polyketide route while gibberellin is synthesized through the isoprenoid pathway [24].

The industrial production of these secondary metabolites is done with cultures of mycelia in liquid (submerged) or solid substrate fermentation. Models of mould growth and metabolic production based on characteristics of mycelial physiology are important to understand, design, and control those industrial fermentation processes [23, 25]. In other words these models enable us to obtain information in a practical way, facilitating fermentation analysis, and can be used to solve problems that may appear during the fermentation process.

5.2. Materials and methods

Microorganism and inoculum preparation *Gibberella fujikuroi* (Sawada) strain CDBB H-984 maintained on potato dextrose agar slants at 4 °C and sub-cultured every 2 months was used in the present work (Culture collection of the Department of Biotechnology and Bioengineering, CINVESTAV-IPN, Mexico). Fully developed mycelia materials from a slant were removed by adding an isotonic solution (0.9% NaCl). The removed mycelium was used to inoculate 300 ml of fresh culture medium contained in an Erlenmeyer flask. The flask was placed in a radial shaker (200 rev min^{-1}) for 38 h at 29 ± 1°C. Subsequent to this time; the contents of the flask were used to inoculate the culture medium contained in the airlift bioreactor. The culture medium employed for the inoculum preparation is reported by Escamilla [26].

http://dx.doi.org/10.5772/53711

5.3. Batch culture in the airlift bioreactor

An airlift bioreactor (Applikon, Netherlands, working volume, 3.5 l) was employed in the present work (Fig 3). It consists of two concentric tubes of 4.0 and 5.0 cm of internal diameter with a settler. The air enters the bioreactor through the inner tube. A jacket filled with water allowing temperature control surrounds the bioreactor. It is also equipped with sensors of pH and dissolved oxygen to control these variables. Moreover it allows feed or retiring material from the bioreactor employing peristaltic pumps.

During the fermentation period, the pH was controlled to 3.0, temperature to 29 °C and aeration rate to 1.6 volume of air by volume of media by minute (vvm). These conditions promoted Bikaverin production with the studied strain were optimized values [26]. About 30 ml subsamples were withdrawn from the bioreactor at different times and were used to perform rheological studies. Biomass concentration was quantified by the dry weight method.

Figure 3. Airlift bioreactor used for the process for Bikaverin production

5.4. Batch culture in the airlift bioreactor

Typical culture medium contained glucose (50 g l^{-1}), NH_4Cl (0.75 g l^{-1}) or NH_4NO_3 (1.08 g l^{-1}), KH_2PO_4 (5 g l^{-1}), $MgSO_4.7H_2O$ (1 g l^{-1}) and trace elements (2 ml l^{-1}). A stock solution of the trace elements used contained (g l^{-1}) 1.0 Fe SO_4. $7H_2O$, 0.15 $CuSO_4$. $5H_2O$ 1.0 $ZnSO_4$. $7H_2O$, 0.1 $MnSO_4$ $7H_2O$, 0.1 $NaMoO_4$, 3.0 EDTA (Na_2 salt) 1 l of distilled water, and hydrochloric acid sufficient to clarify the solution (Barrow et al. 1960). During the fermentation period, the pH was controlled to 3.0, temperature to 29 °C and aeration rate to 1.6 v/v/m. These conditions promoted Bikaverin production with the studied strain but they are not optimized values. About 30 ml subsamples were withdrawn from the bioreactor at different times and were used to perform rheological studies. Biomass concentration was quantified by the dry weight method.

5.5. Hydrodynamics and mass transfer studies

Gas holdup was determined in the actual culture medium using an inverted U-tube manometer as described by [27]. Liquid velocities in the riser were determined measuring the time required for the liquid to travel through the riser by means of a pulse of concentrated sulphuric acid using phenolphthalein as an indicator; the same was done for the downcomer.

The mixing time was calculated as the time required obtaining a pH variation within 5% of the final pH value. For doing this, pH variation was followed after injection of a pulse of a concentrated solution of ammonium hydroxide. The volumetric mass transfer coefficient was determined employing the gassing-out method as described elsewhere [28].

5.6. Rheological studies

Rheological studies of fermentation broth were performed in a rotational rheometer (Haake, Model CV20N) equipped with a helical impeller to perform torque measurements. This type of geometry is appropriate when dealing with complex fluids and the measurement methodology is reported by Brito [29]. Rheological results, like hydrodynamics and mass transfer, are given as the average of two replicates for each sample. All the experiments were carried out in triplicate and the results that are presented are an average.

5.7. Results and discussion

5.7.1. Gas holdup

The importance of gas holdup is multifold. The gas holdup determines the residence time of the gas in the liquid and, in combination with the bubble size, influences the gas–liquid interfacial area available for mass transfer. The gas holdup impacts upon the bioreactor design because the total design volume of the bioreactor for any range of operating conditions depends on the maximum gas holdup that must be accommodated [1]. Figure 4 shows the gas holdup (ε) variation with superficial gas velocity in the riser (v_{gr}).

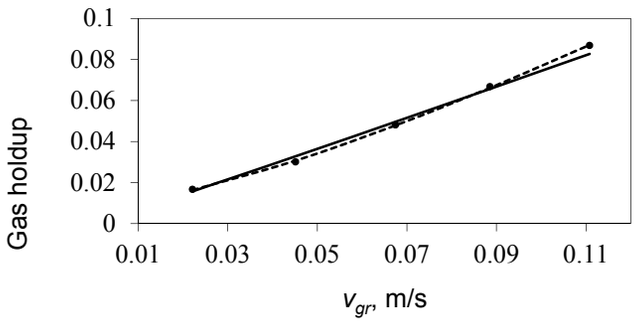

•Experimental data; — Equation 5;—Equation 14

Figure 4.

Figure 4. Gas holdup variation with superficial gas velocity in the riser.

Experimental data were fitted to a correlation of the type of Eq. 5.

http://dx.doi.org/10.5772/53711

$$F = A v_{G_r}^{B} \tag{5}$$

Where F could be the gas holdup (ε), the liquid velocity in the riser (v_{lr}), liquid velocity in the downcomer (v_{ld}) or the volumetric mass transfer coefficient (k_La). This type of correlation has been applied by many investigators (1, 30-33) and was derived empirically. [34] presented an analysis for Newtonian and non-Newtonian fluids where shows the theoretical basis of Eq. 5 (for the gas holdup case). He found that parameters A and B were dependent on the flow regime and on the flow behaviour index of the fluid.

Moreover, parameter A is dependent on the consistency index of the fluid, on the fluid densities and on the gravitational field. Equation 6 was obtained from fitting experimental data.

$$\varepsilon = 0.7980\ v_{gr}^{1.0303} \tag{6}$$

An increase in superficial gas velocity in the riser implies an increase in the quantity of gas present in the riser, that is, an increase of gas fraction in the riser [27, 32]. Chisti, [34] reports a correlation that calculates the value of *B* in Equation 5 (for gas holdup case). The obtained value employing this correlation is 1.2537. Gravilescu and Tudose [32] present a similar correlation, which predicts a value of 0.8434 for *B*. The *B* value obtained in the present work is between the *B* values obtained from these correlations that employ the flow behaviour index obtained from rheological studies. Shah [30] reported that *B* values in Equation 5 oscillate between 0.7 and 1.2.

5.7.2. Liquid velocity

The liquid circulation in airlift bioreactors originates from the difference in bulk densities of the fluids in the riser and the downcomer. The liquid velocity, while itself controlled by the gas holdups in the riser and the downcomer, in turn affects these holdups by either enhancing or reducing the velocity of bubble rise. In addition, liquid velocity affects turbulence, the fluid-reactor wall heat transfer coefficients, the gas-liquid mass transfer and the shear forces to which the microorganism are exposed. Figure 5 shows liquid velocities variation in the riser and the downcomer as a function of superficial gas velocity in the riser.

Liquid velocities in the riser (v_{lr}) and in the downcomer (v_{ld}) were fitted to correlations of the type of Equation 1 and Equations 7 and 8 were obtained.

$$v_{lr} = 1.3335\ v_{gr}^{0.3503} \tag{7}$$

$$v_{ld} = 0.8716\ v_{gr}^{0.2970} \tag{8}$$

Freitas and Teixeira [35] point out that *B* value in equation 7 must be close to 0.3333 for the liquid velocity in the riser since this value was theoretically derived by Kawase [36] and others. The *B* value obtained in the present work (0.3503) is only a little bit higher than 0.3333. Freitas

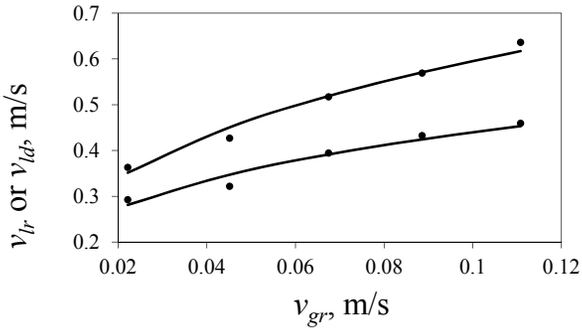

•Experimental data — Equation 7 or 8

Figure 5.

Figure 5. Liquid velocities as a function of superficial gas velocity in the riser.

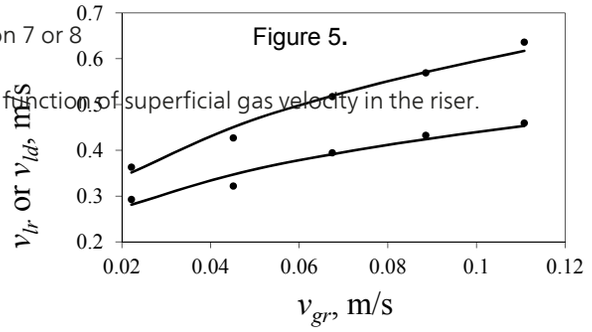

and Teixeira [35] also lowncomer is less than
B value for the liquid obtained in this work.
Liquid velocities in th ncrease in gas velocity
in the riser due to a ls in the riser and the
downcomer.

Figure 5. Liquid velocities as a function of superficial gas velocity in the riser.
• Experimental data —— Equation 7 or 8

Freitas and Teixeira (35) point out that *B* value in equation 7 must be close to 0.3333 for the liquid velocity in the riser since this value was theoretically derived by Kawase (36) and others. The *B* value obtained in the present work (0.3503) is only a little bit higher than 0.3333. Freitas and Teixeira (35) also obtain that *B* value for the liquid velocity in the downcomer is less than *B* value for the liquid velocity in the riser which agrees with the results obtained in this work. Liquid velocities in the riser and in the downcomer increase with an increase in gas velocity in the riser due to an increase in the density difference of the fluids in the riser and the downcomer.

5.7.3. *Mixing time*

Mixing in airlift bioreactors may be considered to have two contributing components: backmixing due to recirculation and axial dispersion in the riser and downcomer due to turbulence and differential velocities of the gas and liquid phases [37](Ch. Mixing time is used as a basis for comparing various reactors as well as a parameter for scaling up [32]. Figure 6 shows the mixing time variation with the superficial gas velocity in the riser.

Once again, the mixing time variation was fitted to a correlation of the type of Equation 5 and Equation 8 was obtained.

Mixing time

Mixing in airlift bioreactors may be considered to have two contributing components: backmixing due to recirculation and axial dispersion in the riser and downcomer due to turbulence and differential velocities of the gas and liquid phases (37)(Ch. Mixing time is used as a basis for comparing various reactors as well as a parameter for scaling up (32)). Figure 6 shows the mixing time variation with the superficial gas velocity in the riser.

Once again, the mixing time variation was fitted to a correlation of the type of Equation 5 and Equation 8 was obtained.

$$t_m = 5.0684\, v_{gr}^{-0.3628} \qquad (9)$$

$$t_m = 5.0684\, v_{gr}^{-0.3628} \qquad (9)$$

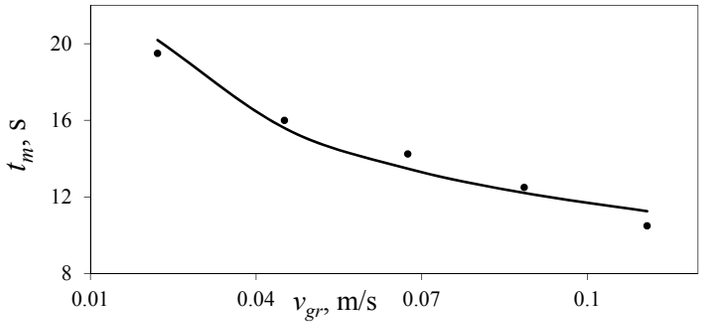

• Experimental data — Equation 5

Figure 6. Mixing time as a function of superficial gas velocity in the riser.

Figure 6. Mixing time as a function of superficial gas velocity in the riser.
• Experimental data —— Equation 5

Choi *et al*., (37) report a *B* value in Equation 5 of –0.36 while Freitas and Teixeira (35) report a *B* value equal to –0.417. The *B* value obtained in this work is similar to the value reported by Choi *et al*., (37). The mixing time decreases with an increase in superficial gas velocity in the riser since the fluid moves more often to the degassing zone where most of the mixing phenomenon takes place due to the ring vortices formed above the draught tube (35).

Volumetric mass transfer coefficient

One of the major reasons that oxygen transfer can play an important role in many biological processes is certainly the limited oxygen capacity of the fermentation broth due to the low solubility of oxygen. The volumetric mass transfer coefficient (k_La) is

http://dx.doi.org/10.5772/53711

Choi *et al*., [37] report a *B* value in Equation 5 of –0.36 while Freitas and Teixeira [35] report a *B* value equal to –0.417. The *B* value obtained in this work is similar to the value reported by Choi *et al*., [37]. The mixing time decreases with an increase in superficial gas velocity in the riser since the fluid moves more often to the degassing zone where most of the mixing phenomenon takes place due to the ring vortices formed above the draught tube [35].

5.7.4. Volumetric mass transfer coefficient

One of the major reasons that oxygen transfer can play an important role in many biological processes is certainly the limited oxygen capacity of the fermentation broth due to the low solubility of oxygen. The volumetric mass transfer coefficient (k_La) is the parameter that characterizes gas-liquid oxygen transfer in bioreactors. One of the commonest employed scale-up criteria is constant k_La. The influences of various design (i.e., bioreactor type and geometry), system (i.e., fluid properties) and operation (i.e., liquid and gas velocities) variables on k_La must be evaluated so that design and operation are carried out to optimize k_La [37].

The value of the volumetric mass transfer coefficient determined for a microbial system can differ substantially from those obtained for the oxygen absorption in water or in simple aqueous solutions, i.e., in static systems with an invariable composition of the liquid media along the time. Hence k_La should be determined in bioreactors which involve the actual media and microbial population [38]. Figure 7 shows the volumetric mass transfer coefficient variation with the superficial gas velocity in the riser.

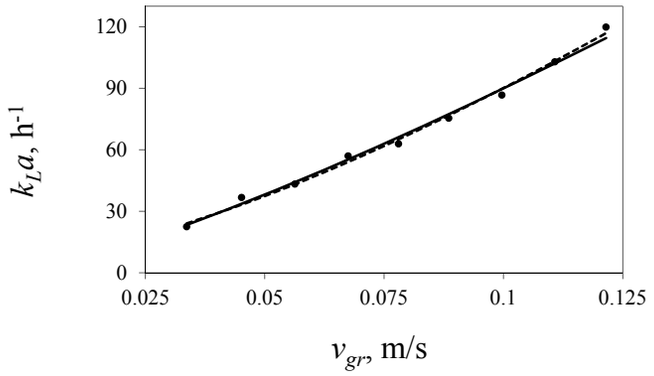

Figure 7

Figure 7. Effect of the superficial gas velocity in the riser on k_La.

Experimental data shown in Figure 7 were fitted to a correlation of the type of Equation 1 and Equation 6 was obtained.

$$k_La = 0.4337\ v_{gr}^{1.2398} \tag{10}$$

[39] report a *B* value in Equation 6 equal to 1.33 and Schügerl *et al*., [40] report a value of 1.58. The value of 1.2398, obtained in this work, is closed to these last values.

Volumetric mass transfer coefficient (k_La) increases with an increase in superficial gas velocity in the riser due to an increase in gas holdup which increases the available area for oxygen transfer. Moreover an increase in the superficial gas velocity in the riser increases the liquid velocity which decreases the thickness of the gas-liquid boundary layer decreasing the mass transfer resistance.

Figure 8 shows the evolution of k_La through fermentation course employing two different nitrogen sources. The k_La decreases in the first hours of fermentation and reaches a minimum value at about 24 hours. After this time the k_La starts to increase and after 48 hours of fermentation it reaches a more or less constant value which remains till the end of fermentation process. This behaviour is similar irrespective of the nitrogen source and will be discussed with the rheological results evidence.

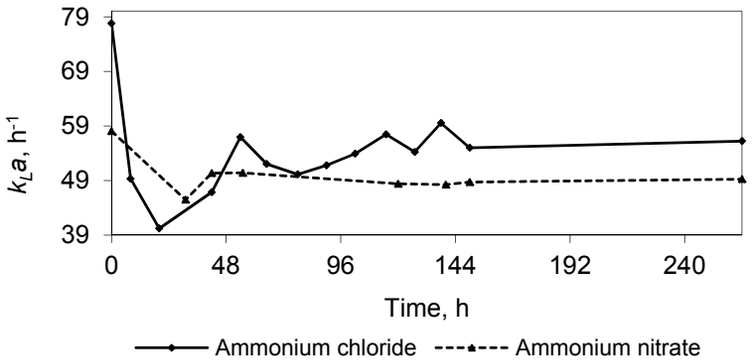

Figure 8. Sthe evolution of k_La through fermentation course employing two different nitrogen sources.

Figure 8

Figure 9 shows the relation between gas holdup and k_La. Mc Manamey and Wase [21] point out that the volumetric mass transfer coefficient is dependent on gas holdup in pneumatically agitated systems. The later was experimentally determined in bubble columns by Akita and Yoshida and other authors [30, 41, 42] they mention that this was expectable since both the volumetric mass transfer coefficient and the holdup present similar correlations with the superficial gas velocity. Mc Manamey and Wase [21] proposed a correlation similar to Equation 1 to relate volumetric mass transfer coefficient with gas holdup. Equation 7 presents the obtained result.

$$k_La = 0.2883\ \varepsilon^{0.9562} \tag{11}$$

Akita and Yoshida [41] and Prokop *et al*. [42] found that the exponent in Equation 7 oscillates between 0.8 and 1.1.

It is well known [16] that logarithmic scale plots of k_La vs. ε/(1- ε) for any particular data set should have a unit slope according to Equation 8.

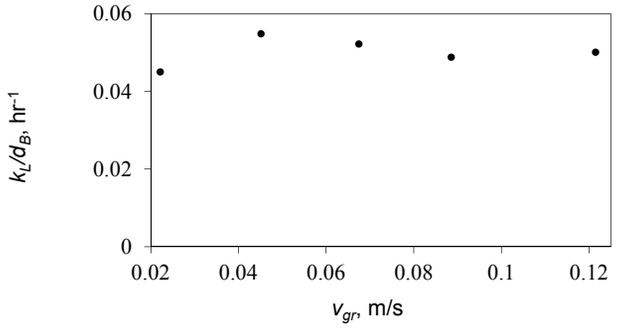

Figure 10. The k_L/d_B ratio as a function of superficial gas velocity.

Figure 8. The k_L/d_B ratio as a function of superficial gas velocity.

The average value of k_L/d_B obtained in the present work is 0.050 s^{-1}. Chisti (27) performed a similar analysis for 97 data points obtained from several different reactors and found an average value of 0.053 s^{-1}. The foregoing observations have important scale-up implications. In large industrial fermenters the k_La determination is not only difficult, but there is uncertainty as to whether the measured results reflect the real k_La or not. The gas holdup measurements on these reactors are relatively easy to carry out, however. Thus, Equation 9 can help to estimate k_La in these reactors once holdup measurements have been made (1).

$$\ln k_L a = \ln\left(6\frac{k_L}{d_B}\right) + \ln\frac{\varepsilon}{(1-\varepsilon)} \tag{12}$$

Where k_L is the mass transfer coefficient and d_B is the bubble diameter. Even though the latter is a generally known fact, few investigators determined these slopes for their data to ascertain the validity of their experimental results. Figure 10 shows this analysis for the experimental data of the present work obtaining a slope of 1.034. Chisti [16] shows the same analysis for two different data set and obtained slopes of 1.020 and 1.056.

Rheology

Rheological parameters such as the flow index (n) and the consistency index (K) depend on such factors as the concentration of solids in the broth, the morphology (length, diameter, degree of branching, shape) of the particles, the growth conditions (flexibility of cell wall and particle), the microbial species and the osmotic pressure of the suspending liquid, among others possible factors.

For the case of mycelia cultures, as the biomass concentration increases the broth becomes more viscous and non-Newtonian; leading to substantial decreases in oxygen transfer rates. This effect is often important since for many aerobic processes involving viscous non-Newtonian broths oxygen supply is the limiting factor determining bioreactor productivity (43). Apparent viscosity is a widely used design parameter which correlates mass transfer and hydrodynamic parameters for viscous non-Newtonian systems (44).

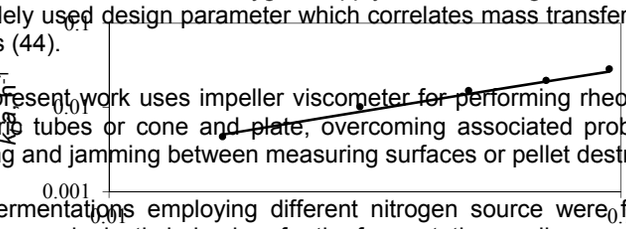

It is worth to mention that the present work uses impeller viscometer for performing rheological studies avoiding the use of other geometries, i.e., concentric tubes or cone and plate, overcoming associated problems with these geometries such sedimentation, solids compacting and jamming between measuring surfaces or pellet destruction (45).

Rheograms obtained for the fermentations employing different nitrogen source were fitted to Ostwald-de Waele model (power law) and in both cases a pseudoplastic behaviour for the fermentative medium was found. Figure 9 shows the results of consistency and flow indexes for these two fermentations where similar results were obtained.

Figure 9. k_La vs. gas holdup

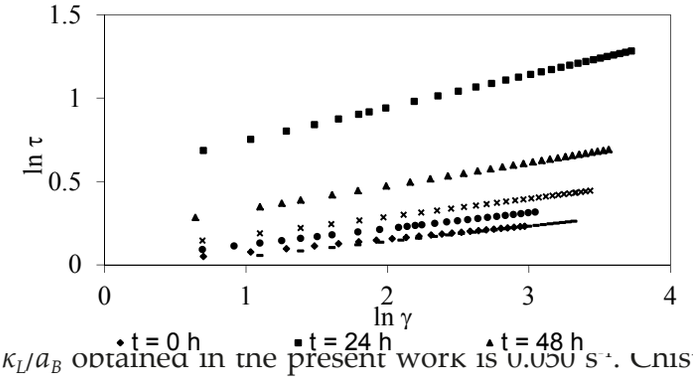

A rearrangement of E[illegible]n in Figure 10

$$\tag{13}$$

The average value of k_L/a_B obtained in the present work is 0.050 s^{-1}. Chisti [27] performed a similar analysis for 97 data points obtained from several different reactors and found an average value of 0.053 s^{-1}. The foregoing observations have important scale-up implications. In large industrial fermenters the k_La determination is not only difficult, but there is uncertainty as to whether the measured results reflect the real k_La or not. The gas holdup measurements

Figure 9. Typical rheogram employing impeller viscometer

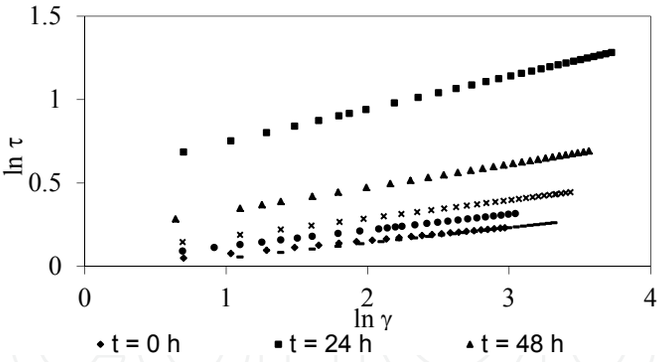

Figure 11.

Figure 11. Typical rheogram employing impeller viscometer.

on these reactors are relatively easy to carry out, however. Thus, Equation 9 can help to estimate k_La in these reactors once holdup measurements have been made [1].

5.7.5. Rheology

Rheological parameters such as the flow index (n) and the consistency index (K) depend on such factors as the concentration of solids in the broth, the morphology (length, diameter, degree of branching, shape) of the particles, the growth conditions (flexibility of cell wall and particle), the microbial species and the osmotic pressure of the suspending liquid, among others possible factors.

For the case of mycelia cultures, as the biomass concentration increases the broth becomes more viscous and non-Newtonian; leading to substantial decreases in oxygen transfer rates. This effect is often important since for many aerobic processes involving viscous non-Newtonian broths oxygen supply is the limiting factor determining bioreactor productivity [43]. Apparent viscosity is a widely used design parameter which correlates mass transfer and hydrodynamic parameters for viscous non-Newtonian systems [44].

It is worth to mention that the present work uses impeller viscometer for performing rheological studies avoiding the use of other geometries, i.e., concentric tubes or cone and plate, overcoming associated problems with these geometries such sedimentation, solids compacting and jamming between measuring surfaces or pellet destruction [45].

Rheograms obtained for the fermentations employing different nitrogen source were fitted to Ostwald-de Waele model (power law) and in both cases a pseudoplastic behaviour for the fermentative medium was found. Figure 11 shows the results of consistency and flow indexes for these two fermentations where similar results were obtained.

During the first 24 hours of fermentation, medium viscosity increases due to exponential growth of mycelia (no lag phase is present) which causes a k_La decrease in Figure 9. After this time, the formation of pellets by the fungus starts to occur reflected in a decrease of medium viscosity and hence an increase in k_La value in Figure 10. After 72 hours of fermentation the medium viscosity was practically unchanged because the stationary growth phase is reached by the fungus reflected in practically constant values of medium viscosity and k_La. With the

http://dx.doi.org/10.5772/53711

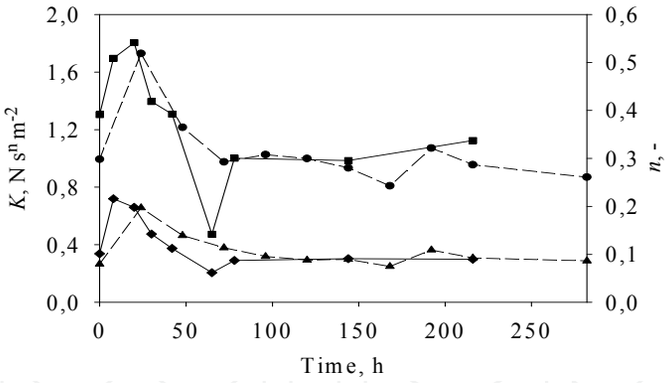

Figure 12

Figure 12. *K* and *n* through fermentation time in the airlift bioreactor.• *K* for ammonium nitrate ▲ *n* for ammonium nitrate ■ *K* for ammonium chloride ◆ *n* for ammonium chloride,

aid of rheological studies is possible to use correlations of the type of Equation 10 to relate holdup and volumetric mass transfer coefficient with fermentation medium viscosity [20, 31, 39, 44] to obtain Equations 12 and 13.

$$F = Av_{gr}^{B}\mu_{app}^{C} \tag{14}$$

$$k_L a = 0.0036\ v_{gr}^{0.3775}\mu_{app}^{-0.5488} \tag{15}$$

$$\varepsilon = 0.0072\ v_{gr}^{0.2381}\mu_{app}^{-0.5703} \tag{16}$$

Figures 2 and 6 show experimental data fitting for holdup and k_La, respectively. As it was expectable, Equations 12 and 13 present a better fit to experimental data than that obtained with the aid of Equations 2 and 3 due to the existence of an extra adjustable parameter.

As can be seen in Fig. 13, there is no lag phase and exponential growth of mycelia starts immediately and ceases during the first 24 h of fermentation. The later causes the medium viscosity to increase (K and n increase in Fig. 12), which causes a k_La decrease in Fig. 6. After 24 h of fermentation, the formation of pellets by the fungus starts to occur, reflected in a decrease of medium viscosity (K and n start to decrease in Fig. 12) and hence an increase in k_La value in Fig. 5. After 72 h of fermentation the medium viscosity was practically unchanged (K and n remain constant in Fig. 12) because the stationary growth phase is reached by the fungus reflected in practically constant values of medium viscosity and k_La. Also, after 72 h of fermentation, the pellet formation process by the fungus stops.

Figure 13 shows the correlation between consistency and flow indexes with biomass concentration. Experimental data were fitted to Eqs. 12 and 13 proposed in the present work. Optimized values for constants in Eqs. 12 and 13 are summarized in Table 1.

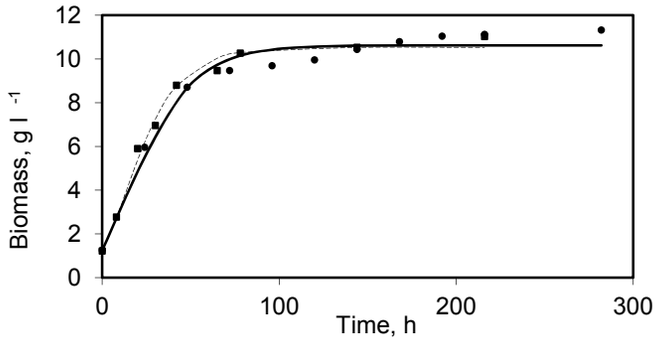

Figure 13

Figure 13. Growth kinetics employing ammonium chloride (◆) or ammonium nitrate (•) as nitrogen source.

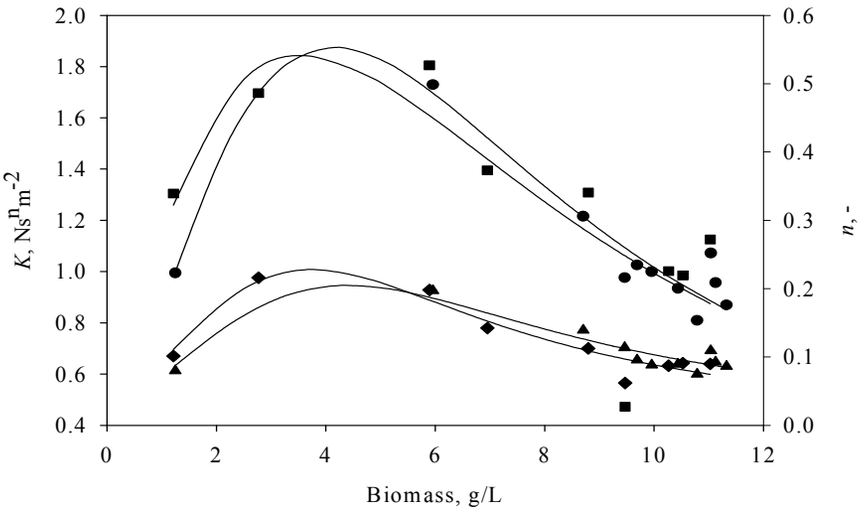

re 14

Figure 14. *K* and *n* as a function of biomass concentration in the airlift bioreactor. • *K* for ammonium nitrate ▲ *n* for ammonium nitrate ■ *K* for ammonium chloride ◆ *n* for ammonium chloride

$$K = \frac{c_1}{\left(1 + \frac{c_2}{x}\right) + \left(\frac{x}{c_3}\right)^2} \tag{17}$$

$$n = \frac{c_1}{\left(1 + \frac{c_2}{x}\right) + \left(\frac{x}{c_3}\right)^2} \tag{18}$$

With the aid of rheological studies is possible to use correlations of the type of Equation 14 to relate gas holdup and volumetric mass transfer coefficient with fermentation medium viscosity [20, 31, 39, 44] to obtain Equations 15 and 16.

http://dx.doi.org/10.5772/53711

$$F = Av_{gr}^{B}\mu_{app}^{C} \tag{19}$$

$$k_L a = 0.0036\ v_{gr}^{0.3775}\mu_{app}^{-0.5488} \tag{20}$$

$$\varepsilon = 0.0072\ v_{gr}^{0.2381}\mu_{app}^{-0.5703} \tag{21}$$

Figures 2 and 5 show experimental data fitting for gas holdup and $k_L a$, respectively. As it was expectable, Eqs. 15 and 16 present a better fit to experimental data than that obtained with the aid of Eqs. 2 and 3 due to the existence of an extra adjustable parameter.

5.8. Conclusions

In the present work preliminary hydrodynamics, mass transfer and rheological studies of Bikaverin production in an airlift bioreactor were achieved and basic correlations between gas holdup, liquid velocity in the riser, liquid velocity in the downcomer, mixing time and volumetric mass transfer coefficient with superficial gas velocity in the riser were obtained.

Adjustable parameters calculated for each variable were compared with literature reported values and a good agreement was obtained.

The gassing out method was successfully applied in determining volumetric mass transfer through fermentation time employing two different nitrogen sources. Irrespective of the nitrogen source the volumetric mass transfer behaviour was similar and it was explained in terms of the fungus growth and changes in its morphology, which affect the culture medium rheology.

Pellet formation by the fungus was used to explain the increase of $k_L a$ or the decrease of medium viscosity. In both fermentations, $k_L a$ decreases as exponential growth of the fungus occurs and reaches an asymptotic value once the stationary growth phase is reached. A helical impeller was employed successfully for rheological studies, avoiding problems of settling, jamming or pellet destruction, finding that the culture medium behaves as a pseudoplastic fluid. Rheological measurements were used to correlate gas holdup and $k_L a$ with apparent culture medium viscosity. Once again, for both fermentations, apparent viscosity increases as exponential growth of the fungus occurs and reaches an asymptotic value once the stationary growth phase is reached.

A satisfactory validation of experimental data for gas holdup and volumetric mass transfer coefficient was performed which allows the employment of these data in scale-up strategies.

6. Case 2: Studies on the kinetics, oxygen mass transfer and rheology in the l-lysine prodution by *Corynebaterium glutamicum*

6.1. Introduction

The industrial application of amino acids in broiler feed has a long history, from the late 1950's have been used to increase the efficiency of the food they eat these animals. Lysine is one of these amino acids to its importance as a feed additive for pigs and poultry, is that it increases the willingness of proteins, bone growth, ossification and stimulates cell division.

Lysine used as an additive for food, is imported because lysine production nationally not exist. The approximate amount of lysine produced worldwide is 550 000 tons per year and almost everything is produced by international companies. Only in the state of Guanajuato, the estimated demand of 300 tons of lysine [46], so that the implementation of appropriate technology for the production of this important amino acid, reduce production costs of animal feed feedlot to reduce imports and generate jobs in the country [47].

Lysine can be produced by chemical synthesis or by enzymatic or microbiological processes. Lysine for obtaining a chemical synthesis is expensive and inefficient process that also by this method are obtained racemic mixtures of D and L forms must then be processed to obtain the L-form which is biologically active. Microbiological fermentation processes are more efficient and direct methods to be based on the accumulation of amino acid that is excreted by the organism in culture media and / or fermentation containing high sugar concentrations and ammonium ions at neutral pH and under aerobic conditions in crops batches [48].

The most commonly used species for the production of lysine is the *Corynebaterium glutamicum* are employed although *Arthrobacter, Brevbibacterium, Microbacterium and Micrococuus.*

Traditionally, the production process of lysine by microbiological fermentation is carried out in stirred vessels, the characteristics of this type of reactor, sometimes, it is economically inconvenient. A better alternative to this configuration are the airlift reactors, the advantages are: low shear, high-speed transfer of oxygen and good mixing, implying a better mass transfer eliminating concentration gradients of either the medium components, avoiding sedimentation of the cells, thereby creating a more favourable environment for development and maintenance, increasing yields and production of lysine.

6.2. Methodology

Inoculum development. Inoculated to the reactor biomass was obtained from a pre-inoculum of ATCC 21253 in lyophilized strain *Corynebacterium glutamicum*.

Experiments in the bioreactor. The batch fermentations were carried out in a reactor airlift with a working volume of 3.4 litres at 30° C (Fig 15). Dissolved oxygen was monitored with a polarographic electrode. The pH of the culture pH was controlled at 7.0 by addition of a solution of 70% NH_4OH. The bioreactor has a condenser which minimizes the error by evaporation losses. The quantity of biomass was inoculated approximately 10% of the bioreactor working volume and sampled periodically.

http://dx.doi.org/10.5772/53711

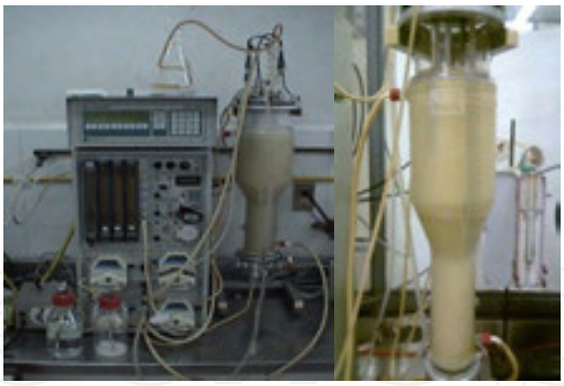

Figure 15. Airlift bioreactor for L-Lysine production

6.3. Mass transfer

For the determination of K_La was used the gas elimination technique [49] and dynamic technique [28]. Measurements for the calculation of K_La by both methods were carried out at 30 ° C and pH 7.0, with a working volume of 3.4 litres of sterile fermentative medium.

Evaluation of the parameters α, β and m_s, the equations were solved using the Runge-Kutta 4th order and an adjustment of the experimental data by nonlinear regression using the GREG program.

The growth rate model is as follows

$$\frac{dX}{dt} = \mu X\left(1 - \frac{X}{L}\right) \tag{22}$$

Where μ is the specific growth rate and L is the maximum value that people can achieve.

The model of product formation rate where the rate of formation is related to the rate of growth:

$$\frac{dP}{dt} = \alpha \frac{dX}{dt} \tag{23}$$

Where α is a constant stoichiometric. In the case where the product is formed independently of the speed of growth:

$$\frac{dP}{dt} = \beta X \tag{24}$$

where β is a proportionality constant. The constant β is similar to the enzyme activity [28]

The substrate consumption model is represented by the following equation:

$$r_S = \frac{r_X}{Y'_{X/S}} + \frac{r_p}{Y'_{P/S}} + m_S X \tag{25}$$

6.4. Results and discussion

The results obtained with the gas elimination technique, allowed calculating the maximum oxygen transfer rate in the system, the dissolved oxygen conditions required.

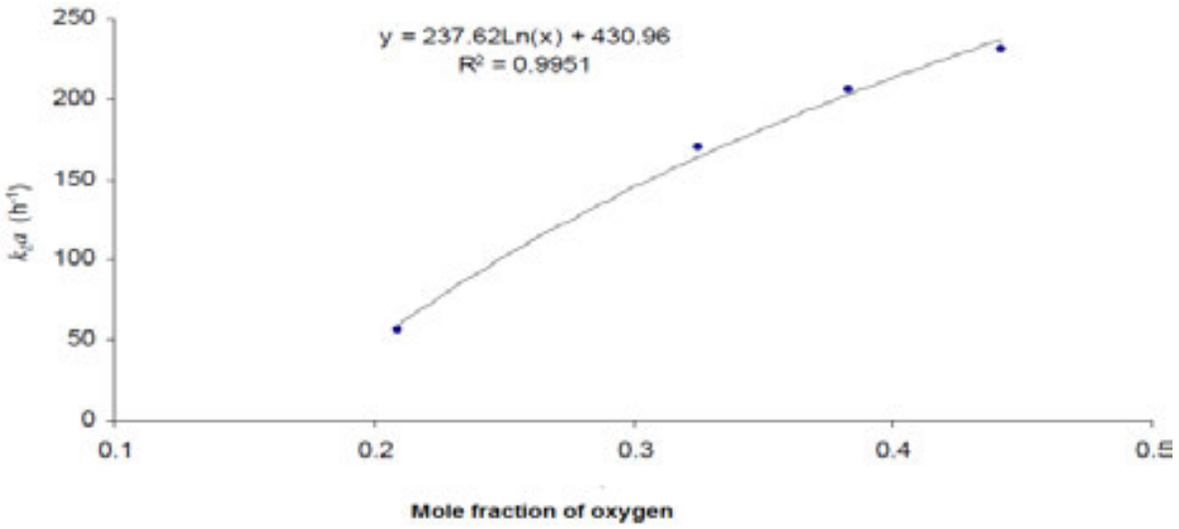

Figure 16. Adjusting $K_L a$ experimental values obtained by the technique of gas removal.

Finding no correlations suitable $K_L a$ experimental data obtained by the technique of gas phase were adjusted to a logarithmic trend line shown in Figure 16.

Figure 17, shows that the production of lysine started between 11 and 12 hours. From 21 up to 46 h the lysine production rate was kept constant (0.385 g / l of lysine h) and declined at 53 h the reduction in production rate was 22% approximately. The overall yield Y_P / S was 0.244 g of lysine / g glucose (at 53 h Y_P / S = 0.223 g lysine / g glucose).

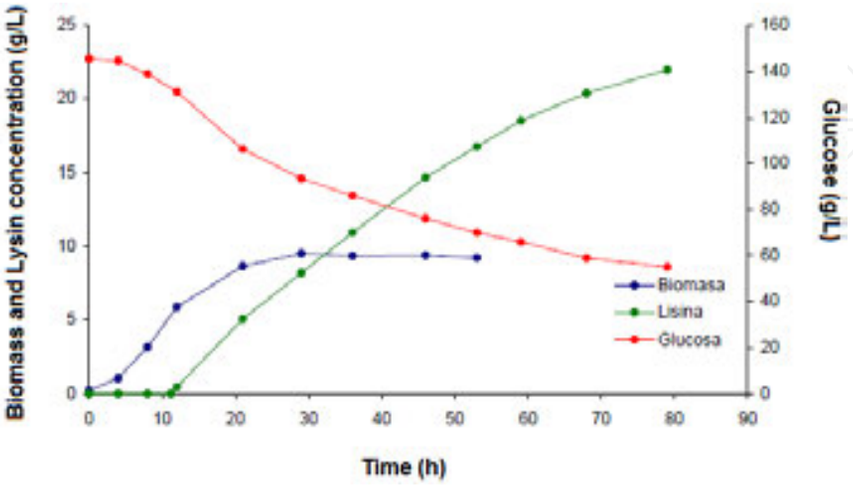

Figure 17. Kinetics of growth, production and consumption with initial glucose 145 g / l.

http://dx.doi.org/10.5772/53711

Parameter	102g/l glucose	145g/l glucose
μ	0.422	0.362
L	11.36	9.26
α	0.974	0.72
β	0.0405	0.0378
Y'X/S	0.42	0.38
Y'P/S	0.36	0.36
ms	–	0.0245

Table 2. Models parameter of growth, production, and lysine and glucose consumption.

In the experiment with 102 g / l initial glucose (Figure 17), lysine production started between 9 and 10 hours. From 22 up to 46 hours the lysine production rate was kept constant (0.475 g / l h of lysine), at 52 hours the reduction in production rate was only 8%. The overall yield Y_P / S was 0.247 g of lysine / g glucose.

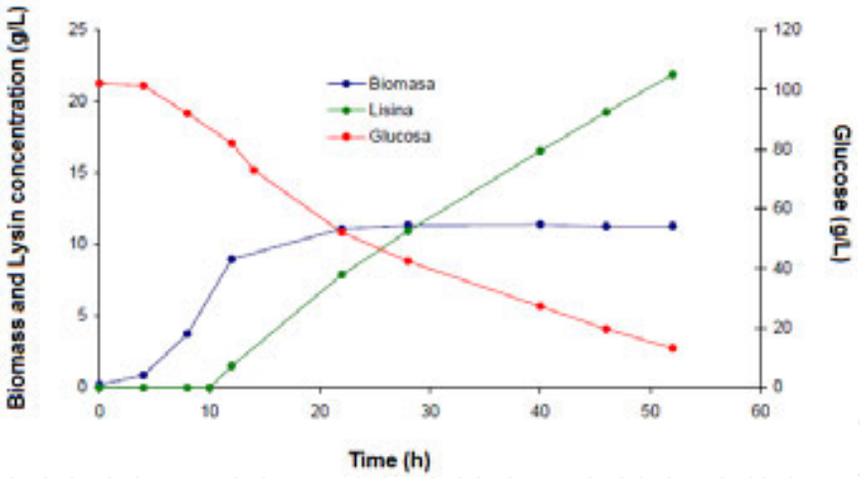

Figure 18. Kinetics of growth, production and consumption with initial glucose 102 g / l.

The model parameters of growth, production and consumption presented in equations [1] to [4] are presented in Table 2.

For evaluation of the parameters α, β and m_s. The equations were solved using the Runge-Kutta 4th order and an adjustment of the experimental data by nonlinear regression using the GREG program [50].

In evaluating the parameters α, β and m_s, the other parameters were kept constant and adjusting the experimental data was performed with the data obtained from 12 h until the end of the maintenance phase (phase to production rate constant).

In Figures 19 and 20 shows the experimental data and the values generated by equations (solid lines) and can be seen that models correctly predict the growth of the microorganism, product formation and substrate consumption from the beginning of the lysine production phase, until the end of the maintenance phase.

Initial Glucose (g/L)	$L - X_0$	μ	$Y_{X/Thr}$	q_{Thr}
145	9.04	0.362	30.1	0.0120
102	11.14	0.422	37.1	0.0114

Table 3. Results obtained from the specified speed of consumption of threonine to two different initial concentrations of glucose.

The rate of consumption of threonine is affected by the initial concentration of glucose due to the effect that the osmotic pressure produced in the cells.

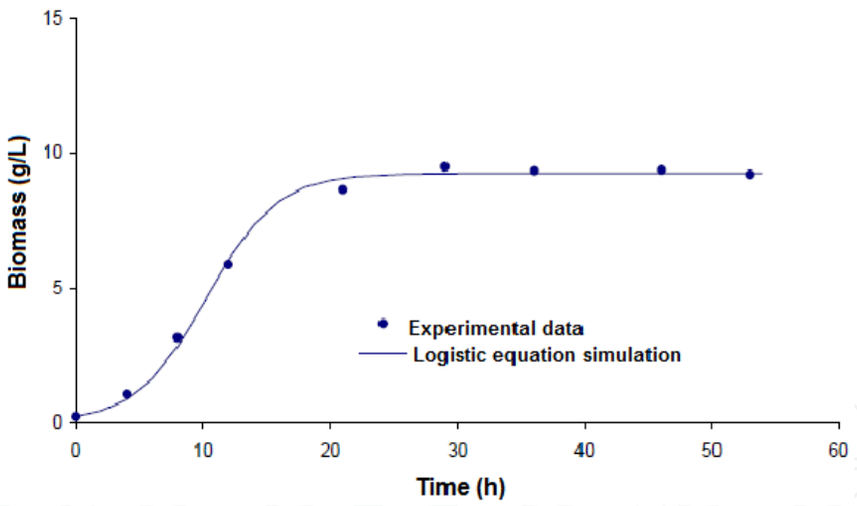

Figure 19. Setting the biomass data to the logistic model (glucose = 145 g/L)

Based on the data in Table 4, an experiment was conducted with airflow of 1 vvm and initial concentration of 150 g / l and 0.6 g / l glucose and L-threonine respectively (Figure 20). The dissolved oxygen began to decrease at approximately 2 h and reached a level below 5% saturation at approximately 20 hours. In Figure 20 it can be seen the effect of oxygen in the growth rate, until 8 h, $\mu = 0.250\ s^{-1}$with a saturation percentage of dissolved oxygen of 20% and 22 to 46, $\mu = 0.0135$, after the culture was oxygen limited.

http://dx.doi.org/10.5772/53711

Air flow (vvm)	ml of antifoam uptake (12 h)	liquid entrained by the air trapped in the condenser
0.5	<1	-
1.0	15	2.2
1.5	27.5	4.4
2.0	55.5	8.0
2.5	>75	11.2
3.0	-	16.8

Table 4. Exploratory experiments for found the optimal initial air flow in the airlift bioreactor.

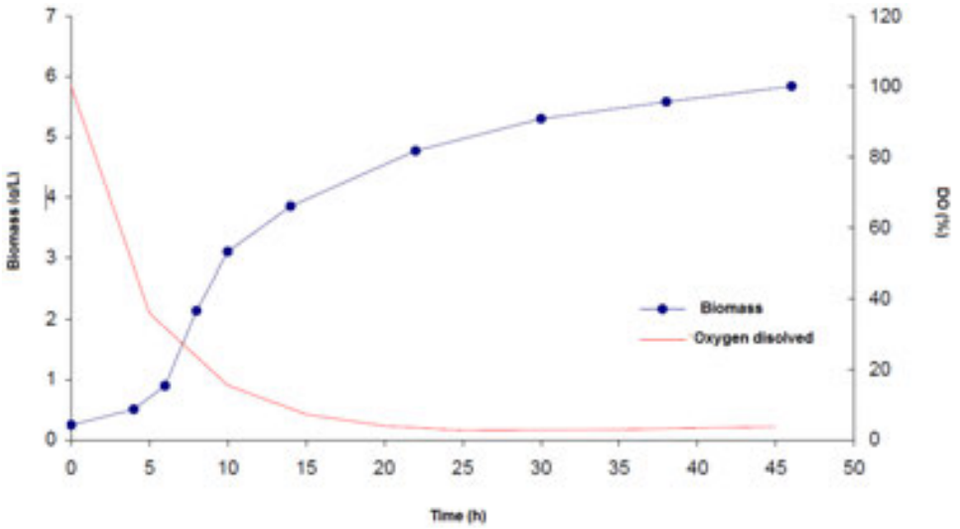

Figure 20. Oxygen limiting effect on the biomass formation.

6.5. Experimental determination of the volumetric coefficient of oxygen transfer

Determination of the solubility of oxygen in the fermentative culture. Because in the experiments with variable air flow was not possible to maintain the dissolved oxygen concentration required for the fermentation experiments was determined by enriching the airflow with oxygen. Were tested for solubility of oxygen in the fermentative culture with various concentrations of glucose, 100, 140 and 180 g / l were obtained the following results:

Glucose (g/l)	DO (%)	MgO_2/l
180	85.22	5.27
140	85.98	5.31
100	87.30	5.40

Table 5. Solubility of oxygen in the fermentative medium with different glucose concentrations.

The difference in concentration of dissolved oxygen concentration between the highest and lowest blood glucose was only 2.11% [51]. Therefore experiments to determine k_La is conducted in fermentative medium with 140 g / l glucose. One way to improve oxygen transfer in the fermentations is to increase the solubility by increasing the mole fraction of gas in the airflow. Based on this, we measured the concentration of dissolved oxygen in the bioreactor by varying the mole fraction of oxygen in the air flow. The results are presented in Table 6.

Oxygen flow rate (vvm)	Air flow rate (vvm)	Oxygen molar fraction	mmol O_2/l	mg O_2/l
0	3400	0.209	0.165	5.27
500	2900	0.325	0.255	8.15
750	2650	0.383	0.307	9.81
1000	2400	0.442	0.349	11.18
1500	1900	0.558	0.441	14.10

Table 6. Experimental results of the measurement of dissolved oxygen.

Experimental data of solubility of oxygen, according to Henry's Law can be adjusted to a straight line (Figure 21). These data were used in subsequent calculations.

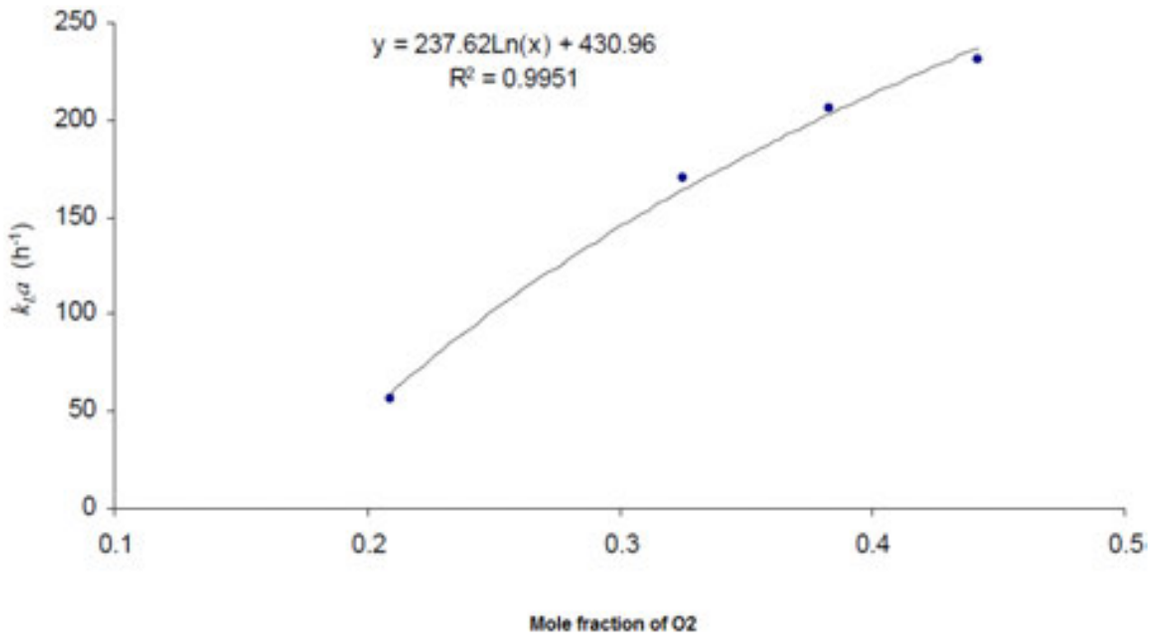

Figure 21. Adjusting k_La experimental values obtained by the technique of gas removal.

In 2003, Ensari and Lim [52] proposed a model in which incorporated the rate of oxygen consumption to describe the kinetics of fermentation of L-lysine and handled 0,266 mmolO_2 /

http://dx.doi.org/10.5772/53711

l as 100% saturation, 30% of this amount is equivalent mgO_2 to 2.55 / l. If we take the value of 2.55 mgO_2 / l, as the minimum value of dissolved oxygen should be maintained during the fermentation and used to calculate the oxygen transfer rate, as the mole fraction of oxygen increases in the air flow, the percentage of dissolved oxygen is reduced, due to the increase in the concentration gradient, which is the driving force for oxygen transfer.

Once the solubility data obtained at different levels of enrichment, we proceeded to calculate the values of the volumetric coefficient of oxygen transfer. K_La value is proportional to the increase in the molar fraction of oxygen in the air flow, this is because increasing the amount of oxygen in the flow, and the contact area is higher. The results obtained with the gas elimination technique, are shown in Table 7 and were useful because together with the values of solubility of oxygen, were used to calculate the maximum oxygen transfer rate in the system, the conditions of dissolved oxygen required.

Mole fraction of oxygen	k_La (h^{-1}]	Number of adjusted data	R^2
0.209	57	10	0.9977
0.209	56	10	0.9979
0.325	171	5	0.9958
0.325	169	5	0.9903
0.383	205	5	0.9921
0.383	208	5	0.9911
0.442	233	3	0.999
0.442	230	3	0.9975

Table 7. Experimental K_La data obtained by the technique of gassing out.

While gassing out method showed a good correlation decided to try the dynamic method to see if you got a better approximation.

6.6. Dynamic method

In Figure 22, shows the data obtained during the development of direct measurements were performed to calculate the volumetric coefficient of oxygen transfer. Data from the first phase of the experiment were used to measure the oxygen consumption rate in the second phase, the coefficient of volumetric oxygen transfer. In fermentation, the oxygen transfer rate can be calculated using the following equation:

$$\frac{dC_L}{dt} = K_L\, a\left(C_L^* - C_L\right) - Q_{O_2}X \tag{26}$$

Where, Q_{O2} is the specific rate of oxygen consumption, which can be defined as the specific growth rate between the yields of oxygen.

$$Q_{O_2} = \frac{\mu}{Y_{O_2}} \tag{27}$$

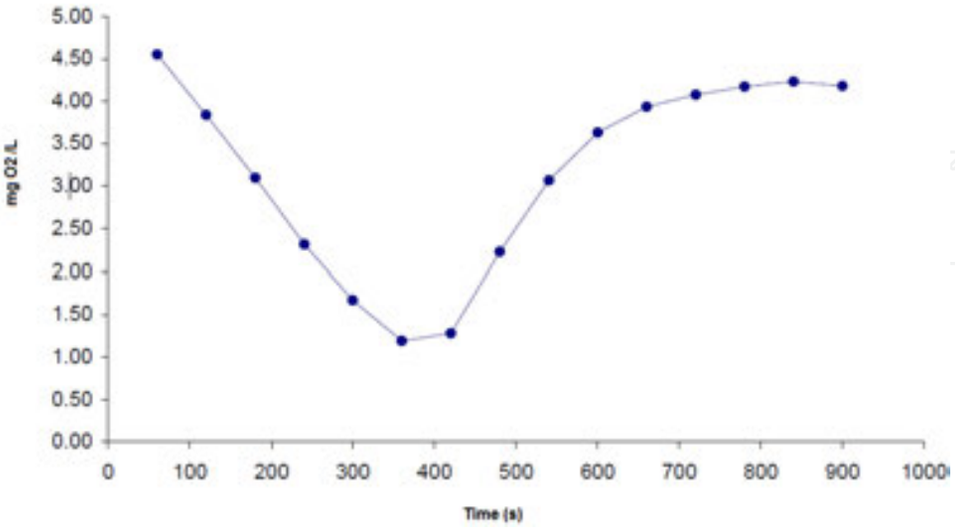

Figure 22. Typical response during the development of the dynamic technique of oxygen uptake

Q_{O2} value can be considered constant during the exponential phase of growth, since, during this stage, both the specific growth rate and yield of oxygen remained constant [25].

This dependency has been used by several authors [51, 53] for correlating the concentration of biomass and the rate of oxygen consumption by a constant parameter, at least during the exponential growth phase. For these experiments, we used a concentration we used a concentration of 140 g / l glucose and the flow of air not enriched with oxygen. The results of calculating the specific rate of oxygen consumption are shown in Table 8. The average value of Q_{O2}, was 159 mg O_2 / g of cells per h, with a standard deviation of 1,414. With this information it is possible to determine the amount of oxygen required for a given biomass concentration in a fermentation and establish the amount of oxygen to be provided shall in the airflow.

Molar fraction molar of Oxygen	$Q_{o2}X$	R^2	X (g cells)	Q_{o2} (mgO_2/g cell h)
0.209	0.01242	0.999	0.28	160
0.209	0.01443	0.997	0.33	158

Table 8. Calculation of the specific rate of oxygen consumption

To calculate the volumetric coefficient of oxygen transfer, we generated a graph (Figure 23) of dC / dt + $Q_{O2}X$ against C_L, where the slope of the line is -1/k_La and intercept and C_L. k_La value of the average between the two experiments was 53 with a standard deviation of 1.414 that show a good acceptation.

http://dx.doi.org/10.5772/53711

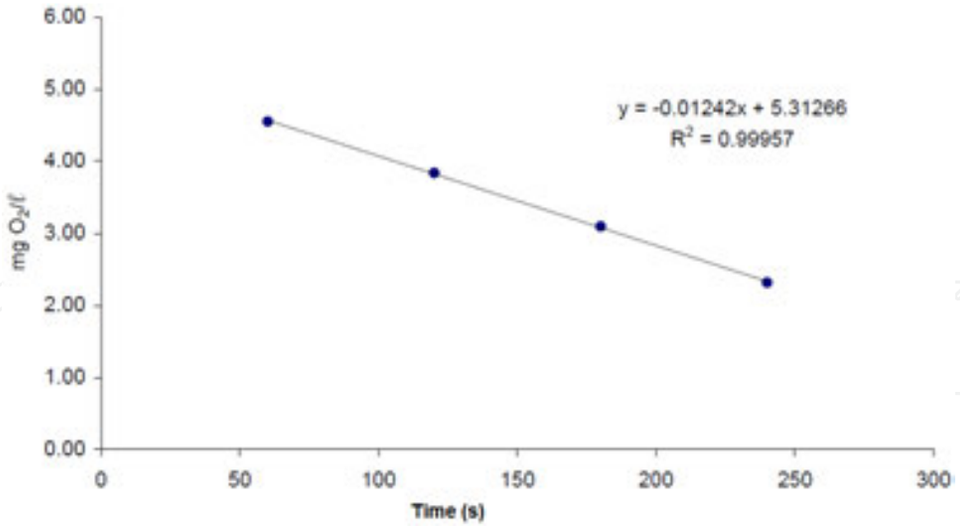

Figure 23. Calculation of the oxygen consumption rate using a direct method, the slope of the line is equal to-$Q_{O2}X$.

Comparing the values obtained with the technique k_La gas removal and direct measurement shows that the k_La value measured in the early hours of the fermentation is very similar to the calculated half fermentative bacteria free. Therefore, to calculate the oxygen transfer rate was determined considering constant since the viscosity during the fermentation does not vary significantly. The solubility of oxygen, may be affected if, therefore, the dissolved oxygen electrode was calibrated at the start of fermentation to a high saturation conditions chosen and the operation of the fermenter was held at the level of dissolved oxygen concentration corresponding.

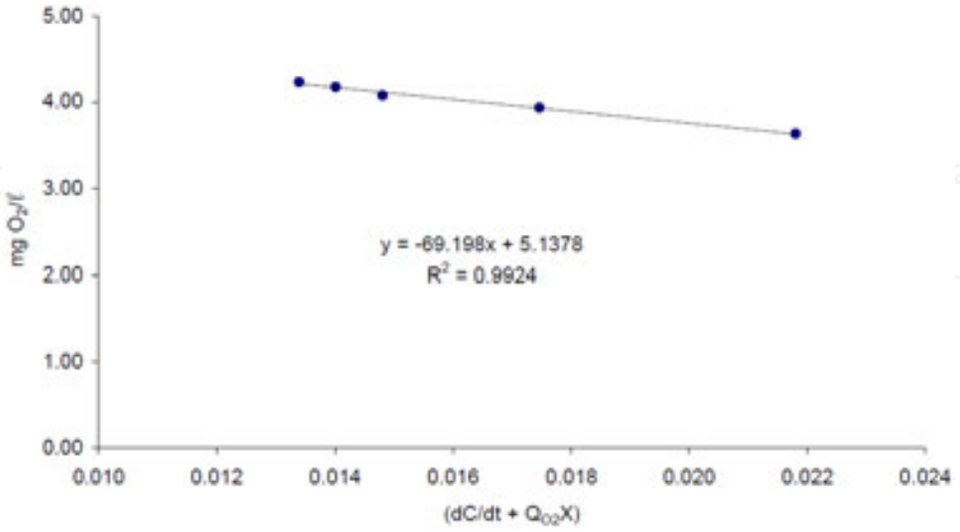

Figure 24. Calculating the volumetric coefficient of oxygen transfer, using a direct method, the slope of the line is equal to -1/k_La.

6.7. Oxygen enrichment experiments

In the case of the 21253 strain of *Corynebacterium glutamicum*, the course of the airlift fermentation in the bioreactor can be divided in 4 phases. The first phase is characterized by exponential growth of the organism (as long as there are no restrictions of any nutrient). The duration of this phase depends on the initial concentration of threonine in the fermentative medium. The depletion of threonine, the second phase begins. At this point lysine production begins, the dissolved oxygen concentration is increased (this implies a decrease in oxygen consumption at the maximum consumption of oxygen is given up to the point of exhaustion), the cell concentration continues to increase and eventually reaches a maximum of approximately 1.6 times the amount shown at the point of exhaustion of threonine 1.7 times [54].

The end of biomass production is due to the depletion of threonine [48] and begins the third phase, in which occurs the maintenance stage and the lysine production rate remains constant. In the fourth phase, the decrease in the production rate is remarkable, because it is not possible cell turnover by the lack of threonine, leucine and methionine, therefore, the biomass concentration decreases.

The yield of threonine should vary depending on the initial concentration of glucose due to growth inhibition that occurs in high concentrations. So far, in experiments with variable air flow, with an initial concentration average of 145 g / l of glucose values were $\mu = 0.331$ (h^{-1}) $Y_X / T_{hr} = 23.10$ (g biomass / g of threonine) and $q_{Thr} = 0.0143$ (g threonine / g biomass h) in the bioreactor airlift was obtained in a yield of 40.50 (g biomass / g of threonine). In both cases the oxygen limited the growth.

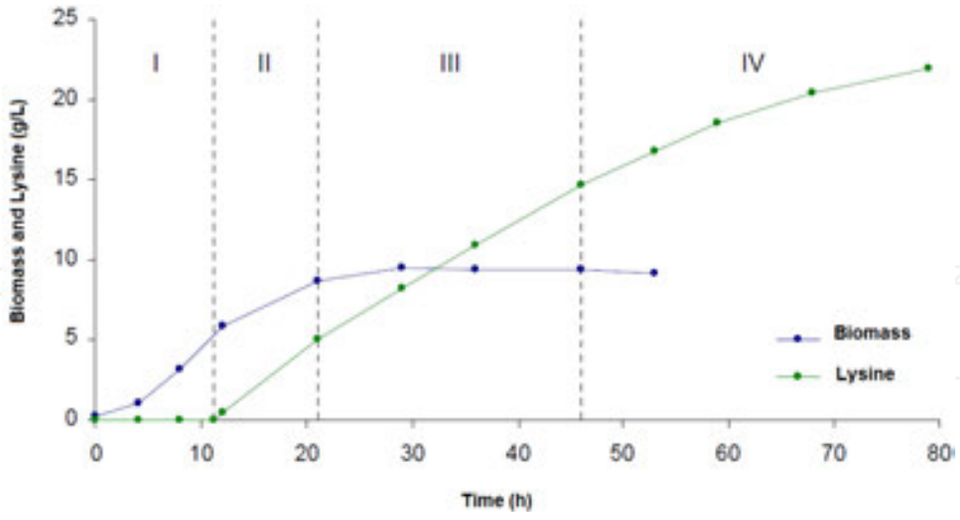

Figure 25. Stages in the lysine fermentation with *Corynebacterium glutamicum* ATCC 21253 in an airlift bioreactor.

To determine the parameters of the model without oxygen limitation were conducted two experiments with initial concentrations of 145 and 100 g / l glucose and 0.3 g / l of threonine. For fermentation with 145 g / l initial glucose, the maximum molar fraction of oxygen was 0.325 and 0.349 for fermentation with 102 g / l initial glucose. In Table 8 shows the final results of

http://dx.doi.org/10.5772/53711

the two fermentations. The kinetics of growth, product formation and substrate consumption can be observed in Figures 26 and 27.

Initial Glucose (g/l)	Biomass (g/l)	Lysine (g/l)	Residual glucose (g/l)	Process time(h)
145	9.26	21.96	55.0	79
102	11.36	21.9	13.2	52

Table 9. Final results of the fermentations with oxygen-enriched air at the same culture conditions.

The yield $Y_{X / Thr}$ between both experiments varied due to the inhibition caused by the initial concentration of glucose, for the experiment with 145 g / l initial glucose Y_X / T_{hr} = 30.13 (g biomass / g of threonine) and in which was used 102 g / l initial glucose was 37.1 (g biomass / g of threonine). This indicates that the amount of threonine to increase relative to the amount of glucose for an adequate quantity of biomass in each fermentation and minimize residual glucose concentrations.

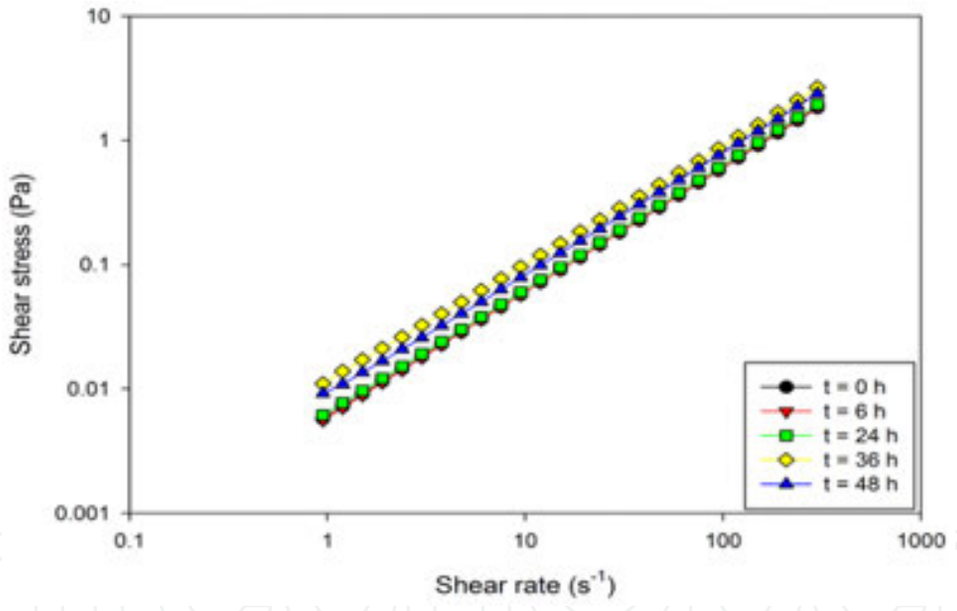

Figure 26. Rheological behaviour when the shear stress versus the shear stress change respect the times and with initial glucose concentration of 100 g / L.

6.8. Results of dynamic rheological behaviour of fermentation process

The model that best described the shear stress in function of the shear rate was

Biofluido behaviour in initial concentrations of 100 (Exp. 1), 140 (Exp. 2) and 180 g / l (Exp. 3) glucose and 1 vvm of air flow, presents different behaviour with respect to its apparent viscosity. Analyses were performed on a controlled stress rheometer with ARG2 type concentric cylinder geometry and with an observation range of 0.1 to 300 rps. The following figures

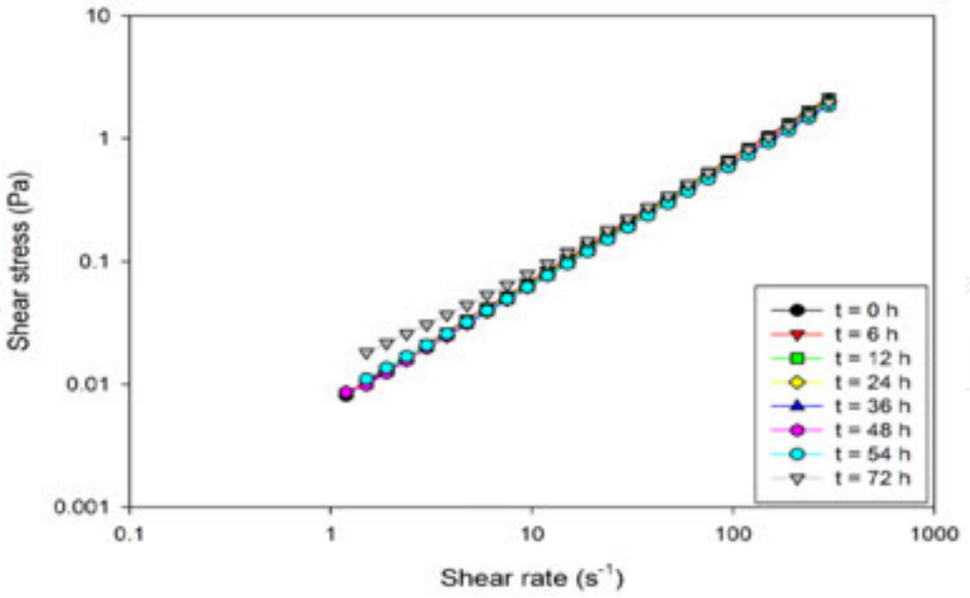

Figure 27. Rheological behaviour when the shear stress versus the shear stress change respect the times and with initial glucose concentration of 140 g / L.

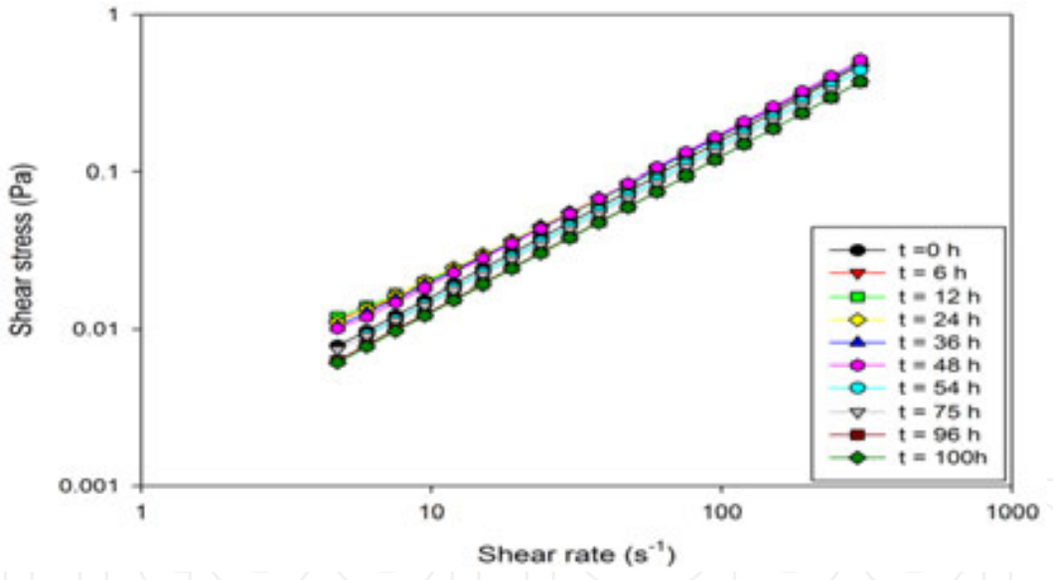

Figure 28. Rheological behaviour when the shear stress versus the shear stress change respect the times and with initial glucose concentration of 180 g / L.

show the behaviour of the shear stress on the shear rate and at different times to take sample of fermentation broth.

The rheological analysis was carried out both in increasing the shear rate and decreasing the same and no significant change was observed i.e. a curve passes over another, this being a feature of pseudoplastic fluids.

http://dx.doi.org/10.5772/53711

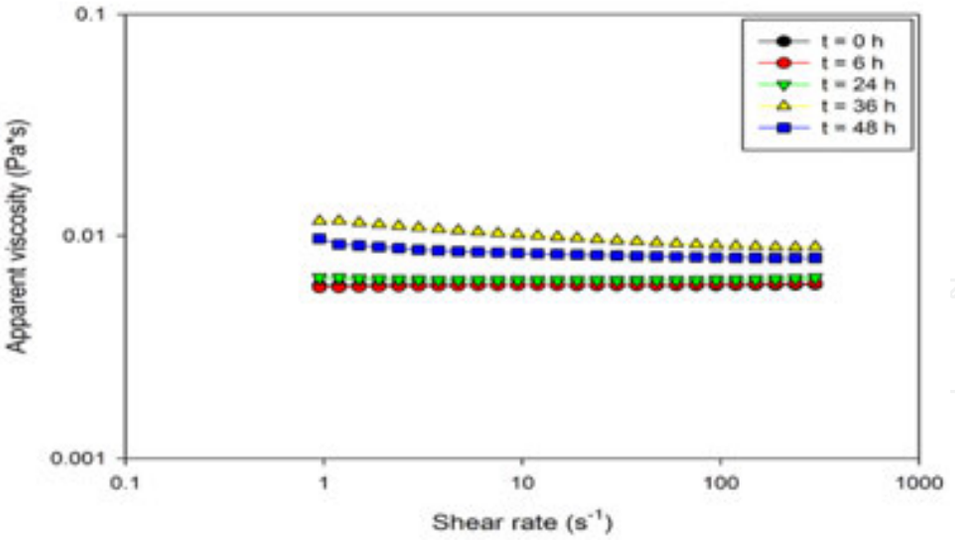

Figure 29. Apparent viscosity versus Shear rate at different times, with initial glucose 100 g / l.

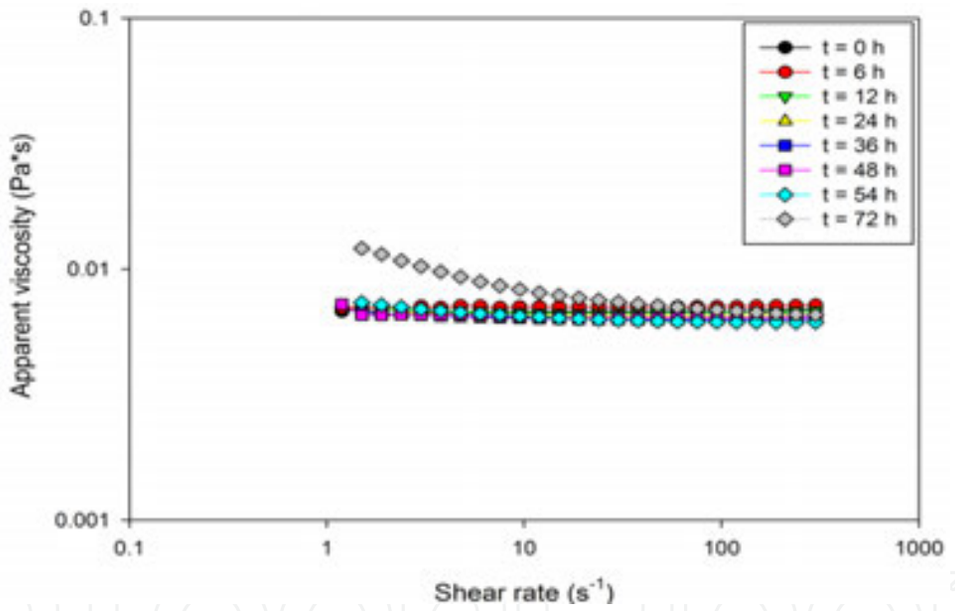

Figure 30. Apparent viscosity versus Shear rate at different times, with initial glucose 140 g / l.

It is evident that the maximum apparent viscosity is obtained between 24 and 36 hours the fermentation process, and subtly observed as the shear stress decreases with increasing the initial concentration of glucose in the medium (Figure 28) for the same shear rate.

The following graphs we can provide additional information to what occurs with respect to the apparent viscosity of the medium and in the same manner at different initial values of glucose.

Similarly one can conclude that the reduced carbon source leads to a decrease in apparent viscosity. The rheological parameters can be described in terms of the model of power law

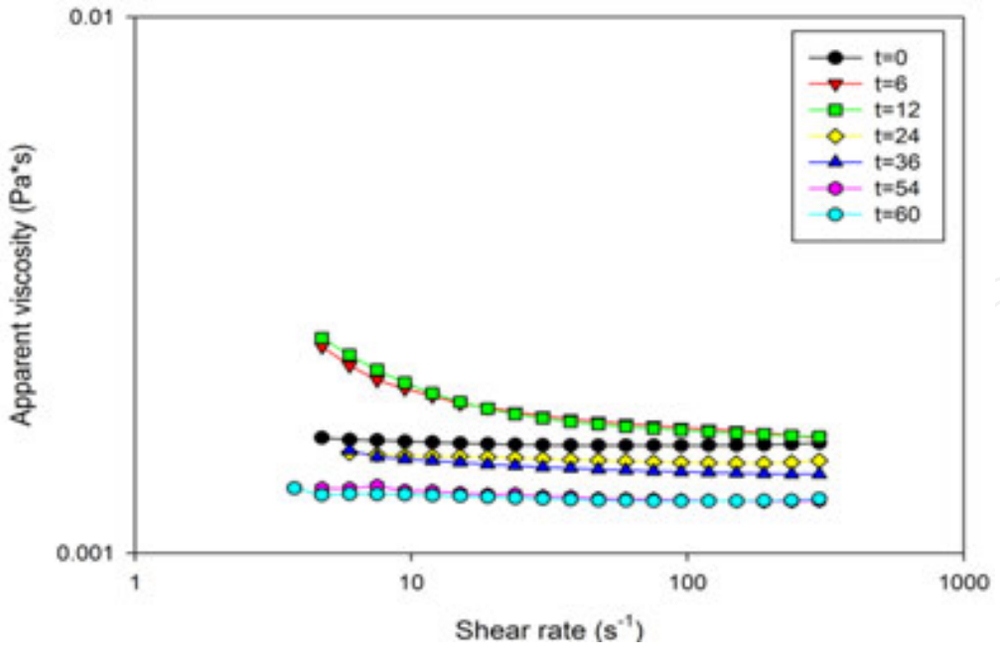

Figure 31. Apparent viscosity versus Shear rate at different times, with initial glucose 180 g / l.

fluids for pseudoplastic, which show a nonlinear relationship between shear stress (τ) and shear rate (γ).

$$\tau = k^{*}\gamma^{n} \tag{28}$$

The constant k is a measure of the consistency of the fluid consistency index is called, and the exponent n is indicative of the deviation of the fluid flow about the behaviour and often called Newtonian behaviour index. For pseudoplastic fluids it holds that n <1, while n> 1 means a dilatant flow behaviour. The power law representing the Newtonian fluid when n = 1. To look more closely shown in the following tables the evolution of the flow rate and consistency index with respect to time and the initial glucose concentration.

Time (h)	K (Pa*s)	n
0	0.00509	1.0055
6	0.00580	1.0111
24	0.00599	1.0136
36	0.01010	0.9779
48	0.00827	0.9926

Table 10. Evolution of the flow and consistency index when were used the initial glucose 100 g / l.

http://dx.doi.org/10.5772/53711

Time (h)	K (Pa*s)	n
0	0.00640	1.0141
6	0.00682	1.0093
12	0.00320	1.0133
24	0.00625	1.0095
36	0.00620	1.0033
48	0.00626	1.0048
54	0.00638	0.9929
72	0.00864	0.9514

Table 11. Evolution of the flow and consistency index when were used the initial glucose 140 g / l.

Time (h)	K (Pa*s)	n
0	0.00157	1.0028
6	0.00209	0.9577
12	0.00202	0.9633
24	0.00227	0.9389
36	0.00212	0.9589
48	0.00199	0.9735
54	0.00152	0.9944
72	0.00149	0.9891
96	0.00133	0.9889
102	0.00126	0.9995

Table 12. Evolution of the flow and consistency indices when were used the initial glucose 180 g / l.

With these data it is easy to see how the cross breeding ground of a pseudoplastic to dilatant, if however it remains very close to the threshold of Newtonian behaviour.

Trying to interpret which may be the kinetic relationship with the following graphs are presented, which illustrates the behaviour of the indices of both flow and consistency.

Can be seen from the graph that during the growth phase of the microorganism fluid behaves as pseudoplastic and when it reaches the stationary phase changes dilatant. The interesting thing is that presented in this final stage the culture broth is such that can be separated easily from the microorganism and undesirable solids, providing the following extraction step of the lysine.

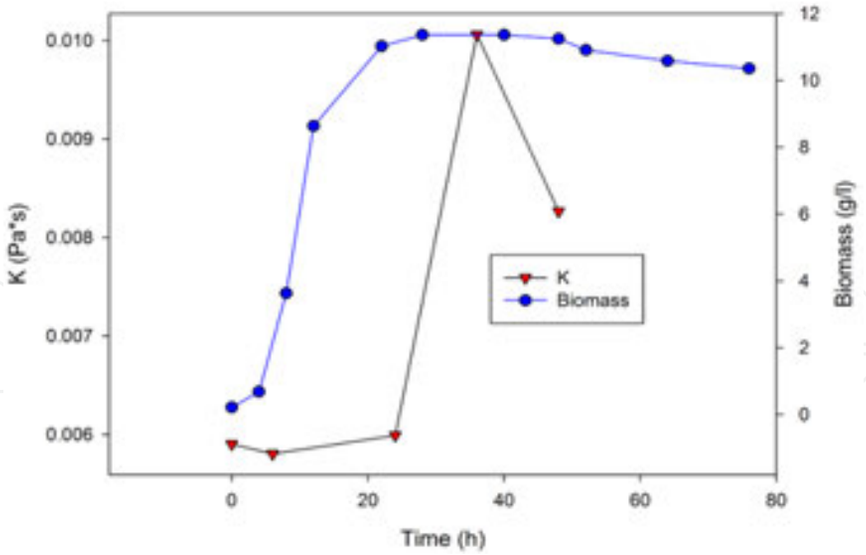

Figure 32. Behaviour consistency index (k) and biomass through fermentation time, using an initial glucose concentration of 100 g / l.

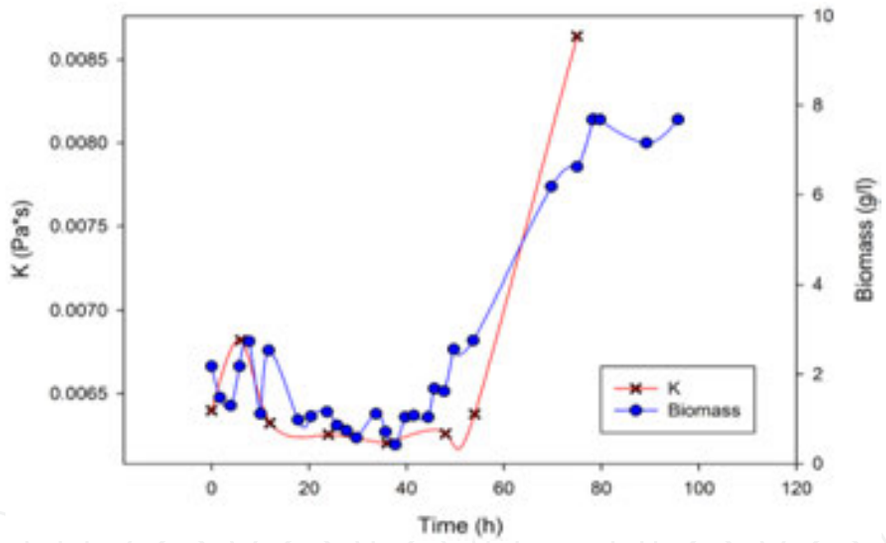

Figure 33. Behaviour consistency index (k) and biomass through fermentation time, using an initial glucose concentration of 140 g / l.

Shows the effect of glucose on the growth of the microorganism, presenting a catabolic repression, and which manifests itself in changing the rheology of the system. We can see that it is present a phase lag increased with increasing initial glucose concentration and the fluid is Newtonian behaviour.

When using the higher initial glucose concentration shows a higher apparent viscosity and thus shows the suppressive effect on growth of the microorganism, once decreases the concentration of glucose over time changes the rheological behaviour of the system, but with a low lysine production.

http://dx.doi.org/10.5772/53711

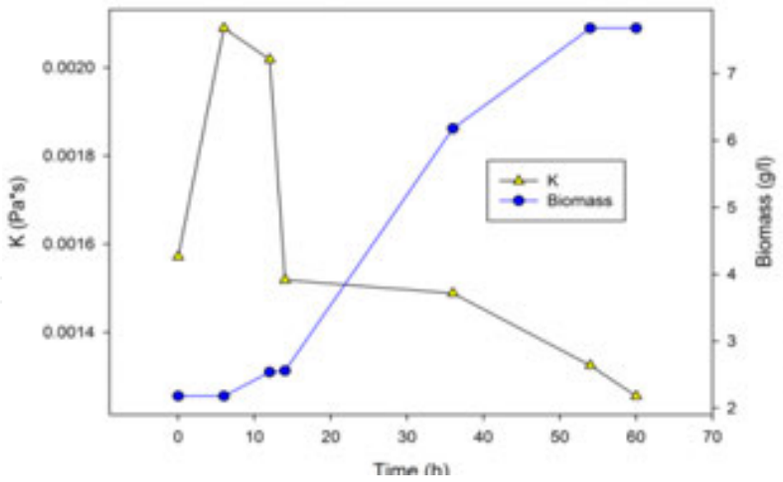

Figure 34. Behaviour consistency index (k) and biomass through fermentation time, using an initial glucose concentration of 180 g / l.

With this new information becomes more evident that the media has a high apparent viscosity at about 24 hours of fermentation, if this information is compared by the kinetics osmolality can be concluded to be due to agglomeration of biomass and the relative glucose in the medium.

Similarly one can conclude that the reduced carbon source leads to a decrease in apparent viscosity. The rheological parameters can be described in terms of the model of power law fluids for pseudoplastic, which show a nonlinear relationship between shear stress and shear rate.

7. Conclusions

Using the obtained relationships between amino acids were prepared culture media in which, L-threonine limits growth and the amino acids L-leucine and L-methionine is not present in excess, reducing the cost of these amino acid supplementation. The initial concentrations of threonine and glucose, affect the growth of the microorganism. The lack of threonine causes a cessation in growth and a subsequent decrease in biomass, while glucose depending on the initial concentration affects the specific growth rate and inhibits the formation of biomass. Thus the overall process yield is closely related to the initial concentrations of threonine and glucose airlift reactors in the oxygen transfer rate can be increased by increasing the air flow. In studies in the present study we observed that, the use of air flows greater than 1 vvm generate a large amount of foam, making it necessary to use defoamers, in decreasing the solubility of oxygen in the fermentative medium. To maintain adequate oxygenation, in combination with the advantages of the airlift bioreactor, resulted in a prolongation of the maintenance phase, whereby the lysine production rate was constant for a period of time greater than that reported in stirred tank bioreactors. In an airlift, using a minor amount of biomass can generate the same or greater amount of product, reducing the initial amount of amino acids, glucose and

ammonium sulfate. Growth models, product formation and substrate consumption correctly predict from the start of the production phase of lysine, to the end of phase constant production rate. It can therefore be used for the simulation of the process from the beginning of fermentation, until the end of the maintenance phase.

Author details

Ana María Mendoza Martínez[1] and Eleazar Máximo Escamilla Silva[2*]

*Address all correspondence to: eleazar@iqcelaya.itc.mx

1 Technological Institute of Madero City, Division of Graduate Studies and Research (ITCM), Madero, México

2 Chemical Departments, Technological Institute of Celaya, Celaya, México

References

[1] Chisti Y, Moo-Young, M. On the calculation of shear rate and apparent viscosity in airlift and bubble column bioreactors. Biotechnol Bioeng. 1989;34:1391-2.

[2] Merchuk JC, Ladwa, N., Cameron, A., Bulmer, M. and Pickett, A. Concentric-tube airlift reactors: Effects of geometrical design on performance. AIChE J. 1994;40:1105-17.

[3] Chisti Y. Pneumatically Agitated Bioreactors in Industrial and Environmental Bioprocessing: Hydrodynamics, Hydraulics and Transport Phenomena. American Society of Mechanical Engineers. 1998;51:33-112.

[4] Joshi J.B. RVV, Gharat S.D., Lee S.S.,. Sparged Loop Reactors. Canadian Journal of Chemical Engineering. 1990;68:705-41.

[5] Petersen E.E. MA. Hydrodynamic and Mass Transfer Characteristics of Three-Phase Gas-Lift Bioreactor Systems. Critical Review in Biotechnology. 2001;21:233-94.

[6] Merchuk JC, Ladwa N., Cameron A., Bulmer M., Pickett A.,. Concentric- Tube Airlift Reactors: Effects of Geometric Design on Performance. AIChE Journal. 1994;40:1105-17.

[7] Gravilescu M, Tudose, R.Z. Modelling mixing parameters in concentric-tube airlift bioreactors. Part I. Mixing time.. Bioprocess Eng,. 1999;20:423-8.

[8] Merchuk JC, Ladwa, N., Cameron, A., Bulmer, M., Pickett, A., Berzin, I. Liquid flow and mixing in concentric tube air-lift reactors. Chem Technol Biotech. 1996;66:172-82.

[9] Merchuk JC, Ladwa, N. Cameron, A. Bulmer, A., Pickett, M. and Berzin, I. Liquid flow and mixing in concentric tube air-lift reactors. Chem Technol Biotech. 1996;66:174-82.

[10] Barnea DT, Y. Fluid Mechanics. In: Cheremisinoff e, editor. Encyclopedia of Fluid Mechanics. Gulf, Houston, Tex., 1986. p. 403-91.

[11] Wallis GB, editor. One Dimensional Two-Phase Flow. New York, : McGraw-Hill; 1969.

[12] Wiswanathan K, editor. Flow Patterns in Bubble Columns. Gulf, Houston, Tex., 1969.

[13] Russell AB, Thomas, C.R., Lilly, M.D.. The influence of vessel height and top section size on the hydrodynamics characteristics of air lift fermenters. Biotechnol Bioeng,. 1994;43:69-76.

[14] Weiland P. Influence of draft tube diameter on operation behaviour of airlift loop reactors. Ger Chem Eng. 1984;7:374-85.

[15] Bello RAR, C.W., Moo-Young, M.. Prediction of the Volumetric Mass Transfer Coefficient in Pneumatic Contactors. Chem Eng Sci,. 1985;40:53-8.

[16] Chisti MY, Moo-Young, M. Airlift reactors: Characteristics, applications and design considerations. Chem Eng Commun,. 1987;60:195-242.

[17] Koide K, Horibe, K., Kawabata, H., Ito, S.,. Gas holdup and volumetric liquid-phase mass transfer coefficient in solid-suspended bubble column with draught tube. J Chem Eng Japan,. 1985;18:248-54.

[18] Merchuk JC, Bulmer, M. Ladwa, N.A., Pickett, M. and Cameron, A, editor. Bioreactor Fluid Dynamics London: Elsevier; 1988.

[19] Siegel MH, Robinson, C.W.,. Applications of airlift gas-liquid solid reactors in biotechnology. Chem Eng Sci 1992;47:3215-29.

[20] Halard B, Kawase, Y., Moo-Young, M.,. Mass transfer in a pilot plant scale airlift column with non-Newtonian fluids.. Ind Eng Chem Res,. 1989;28:243-5.

[21] Mc Manamey WJ, Wase, D.A.J.,. Relationship between the volumetric mass transfer coefficient and gas holdup in airlift fermentors.. Biotechnol Bioeng 1986;28:1446-8.

[22] Merchuk JC, Yunger, R.. The role of the gas—liquid separator of airlift reactors in the mixing process. Chem Eng Sci. 1990;45:2973-5.

[23] Escamilla S, E.M., Dendooven, L., Magaña, I.P., Parra, Saldivar, R., De la Torre, M.. Optimization of Gibberellic acid production by immobilized Gibberella fujikuroi mycelium in fluidized bioreactors. J Biotechnol,. 2000;76:147-55.

[24] Jones A, Pharis, R.P.,. Production of gibberellins and Bikaverin by cells of Gibberella fujikuroi immobilized in carrageenan.. J Ferment Technol,. 1987;65:717-22.

[25] Bailey JE, Ollis, D. F., editor. Transport phenomena in bioprocess systems, Design and analysis of biological reactors. Biochemical engineering fundamentals.. New York: Mc Graw-Hill, ; 1986.

[26] Escamilla S, E.S., Poggi, Varaldo, H., De la torre, Martínez, M., Sánchez, Cornejo, G., Dendooven, L. Selective production of Bikaverin in a fluidized biorreactor with immobilized Gibberella fujikuroi. World J of Microbiol Biotechnol 2001;17:469-74.

[27] Chisti MY, editor. Airlift bioreactor. London-New York: Elsevier Appl. Science, ; 1989.

[28] Quintero RR, editor. Ingeniería bioquímica, Teoría y aplicaciones.. México: Ed. Alambra. ; 1981.

[29] Brito-De la Fuente E, Nava, J.A., López, L.M., Medina, L, Ascanio, G., Tanguy, P.A. Process viscometry of complex fluids and suspensions with helical ribbon agitators. Can J Chem Eng,. 1998;76:689-95.

[30] Shah YT, Kelkar, B.G., Godbole, S.P., Deckwer, W.D.. Design parameters estimations for bubble column reactors.. AIChE J 1982;28:353-79.

[31] Godbole SP, Schumpe, A., Shah, T., Carr, N.L. Hydrodynamics and mass transfer in non-Newtonian solutions in a bubble column.. AIChE J,. 1984;30:213-20.

[32] Gavrilescu M. TRZ. Effects of Geometry on Gas Holdup. Bioprocess Engineering,. 1998;19:37-44.

[33] Abashar M.E. NU, Rouillard A.E., Judd R. Hydrodynamic flow regimes, gas holdup, and liquid circulation in airlift reactors. Ind Eng Chem Res,. 1998;37:1251-9.

[34] Chisti Y, Moo-Young, M. On the calculation of shear rate and apparent viscosity in airlift and bubble column bioreactors. Biotechnol Bioeng,. 1989;34:1391–2.

[35] Freitas C, Teixeira J.A. Hydrodynamic studies in an airlift reactor with an enlarged degassing zone. Bioprocess Engineering. 1998;18:267-79.

[36] Kawase Y. Liquid circulation in external-loop airlift bioreactors.. Biotechnol Bioeng 1989;35:540-6.

[37] Choi KH, Chisti, Y, Moo,Young, M.,. Comparative evaluation of hydrodynamic and gas–liquid mass transfer characteristics in bubble column and airlift slurry reactors. Biochem Eng J,. 1996;62:223-9.

[38] Tobajas M, García, Calvo, E.,. Comparison of experimental methods for determination of the volumetric mass transfer coefficient in fermentation processes. Heat Mass Transfer 2000;36:201-7.

[39] Barboza M, Zaiat M, Hokka, C.O.,. General relationship for volumetric oxygen transfer coefficient (kLa) prediction in tower bioreactors utilizing immobilized cells. Bioprocess Eng,. 2000;22:181-4.

[40] Schügerl KL, J. Oels, U. Bubble column bioreactors. Adv Biochem Eng. 1977;7:1-81.

[41] Akita K Y, F. Gas holdup and volumetric mass transfer coefficient in bubble columns. Effects of liquid properties. Ind Eng Chem Process Des Develop,. 1973;12:76-80.

[42] Prokop A, Janı´k, P., Sobotka, M., Krumphanzi, V.. Hydrodynamics, mass transfer, and yeast culture performance of a column bioreactor with ejector. Biotechnol Bioeng 1983;25:1140-60.

[43] Moo-Young M, Halard, B., Allen, D.G., Burrell, R., Kawase, Y.. Oxygen transfer to mycelial fermentation broths in an airlift fermentor.. Biotechnol Bioeng. 1987;30:746-53.

[44] Al-Masry W.A. DAR. Hydrodynamics and mass transfer studies in a pilot-plant air-lift reactor: non-Newtonian systems. Ind Eng Chem Res,. 1998;37:41-8.

[45] Metz B, Kossen, N.W.F., van Suijdam, J.C.,. The rheology of mould suspensions.. Adv Biochem Eng. 1979;11:103-56.

[46] (INEGI) INdEyG. Demanda de l-Lisina en el estado de Guanajuato. In: Estadistica, editor. Guanajuto2007.

[47] W. L, editor. Amino acids – technical production and use.1996.

[48] Toennies G. Role of aminoacids in postexponential growth.. J Bacteriol 1965;90:438-42.

[49] Van't Riet K. Review of measureing methods and results in nonviscous gas-liquid mass tranfer in stirred vessels. Ind Eng Chem Process Des Develop,. 1979;18:357-64.

[50] Keen RE, Spain, J.D., editor. Computer simulation in biology. Liss. USA: Wiley; 1992.

[51] Singh V. On-line measurements of oxygen uptake in cell culture usig the dynamic method.. Biotechnol Bioeng,. 1996;52:443-8.

[52] Ensari S, Lim, C. H.. Apparent effects of operational variables on the continuous culture of Corynebacterium lactofermentum.. Process Biochemistry 2003;38:1531-8.

[53] Pirt SJ, editor. Principles of microbe and cell cultivation.. London: Blackwell; 1975.

[54] Kiss RD. Metabolic activity control of the L-lisine fermentation by restrained growt fed-batch strategies. Cambridge, MA: M.I.T; 1991.

IntechOpen

IntechOpen